Regularized Wiener–Hopf method in problems modelled by entire unknowns and exponential phase factors: the electromagnetic thick slot

PHILOSOPHICAL TRANSACTIONS A

royalsocietypublishing.org/journal/rsta

Research

Cite this article: Daniele V, Lombardi G. 2025 Regularized Wiener–Hopf method in problems modelled by entire unknowns and exponential phase factors: the electromagnetic thick slot. *Phil. Trans. R. Soc. A* **383**: 20240351.
https://doi.org/10.1098/rsta.2024.0351

Received: 14 February 2025
Accepted: 2 April 2025

One contribution of 20 to a theme issue 'Analytically grounded full-wave methods for advances in computational electromagnetics'.

Subject Areas:
applied mathematics, mathematical physics, wave motion, electromagnetism, computational physics

Keywords:
Wiener–Hopf method, integral equations, Green's function, spectral domain, entire functions, regularization, Fredholm factorization, wave motion, diffraction, electromagnetism

Author for correspondence:
Guido Lombardi
e-mail: guido.lombardi@polito.it

THE ROYAL SOCIETY PUBLISHING

Regularized Wiener–Hopf method in problems modelled by entire unknowns and exponential phase factors: the electromagnetic thick slot

Vito Daniele and Guido Lombardi

DET, Politecnico di Torino, Torino, Italy

GL, 0000-0002-7311-2279

This paper presents an effective method to deal with problems formulated in terms of Wiener–Hopf equations which contain entire unknowns and exponential phase factors. The methodology reduces the factorization problem to regularized integral equations. In particular, we validate the method analysing a practical application in electromagnetism: the scattering of a plane wave by a slot in a thick metallic screen.

This article is part of the theme issue 'Analytically grounded full-wave methods for advances in computational electromagnetics'.

1. Introduction

The Wiener–Hopf (WH) method [1–4] has been systematically extended during the last 10 years to model complex mathematical-physics wave-scattering problems with impact in engineering, see for instance [5–12]. This extension is particularly relevant for the analysis of structures composed of a combination of sub-domains of different shapes, like angular, layered and semi-finite sub-regions made up of complex materials with different constitutive parameters.

The present paper solves the still open (or at least not completely addressed) problem of handling entire unknowns and exponential phase factors in the solution of Wiener–Hopf equations, that are evident starting from the basic problems classified as modified Wiener–Hopf equations or three-part mixed boundary value problems [1–4]. These kinds of unknowns are present each time the Wiener–Hopf method in spectral domain is applied

to scattering problems where the geometry of the problem presents finite penetrable/impenetrable regions, e.g. strips, slots, slits, bricks and cylindrical structures of various shapes that can be staggered with respect to each other.

In fact, the presence of entire functions derives from the application of spectral transformation to quantities defined in limited domain and the exponential phase factors arise prominently in problems with staggered subdomains. These mathematical properties can be easily understood through the application of Laplace or Fourier transformations to physical quantities defined in the considered set of problems.

Several attempts in literature have shown the difficulty of reaching high quality/high precision solutions for this category of Wiener–Hopf problems and in particular solutions are provided for specific problems. The current literature presents methodologies that make reference to the fundamental works inspired by Jones with his popular method to handle modified WH equations [13], works where modified equations are transformed into classical matrix Wiener–Hopf equations [4] and papers by Abrahams's research group originating from [14].

The Jones method reduces the solution of modified equations to implicit Fredholm integral equations that depends on the availability of kernel pre-factorizations and the determination of coefficients via a system of infinite equations due to the presence of poles or branch cuts in the spectra. This method represents a valid first methodology to deal with problems modelled by entire functions and it has been used by several authors with particularized modifications [1–4,13,15–33].

Alternatively, for the specific cases of transversely/longitudinally modified equations, the problem can be reduced systematically and effectively to matrix Wiener–Hopf equations where in the case of longitudinally modified equations the matrix shows exponential phase factors, see §1.5 of [4].

Another technique is proposed in [14] that applies a sampled representation of entire functions in terms of unknown coefficients, whose implementation recalls information theory, which is not directly related to the physics of the problem. The solution procedure for the WH problems requires integral equation formulation and the solution of a system of infinite equations for the samples. The work inspired factorization of a matrix kernel containing exponential phase factors and it is based on the solution of coupled integral equations that can be iteratively performed. The technique has been applied and extended in [34–38].

The present paper reports an innovative, versatile, general, completed, not-specialized effective semi-analytical method to obtain precise solution in arbitrarily general Wiener–Hopf problems defined in spectral domain and containing entire unknowns with exponential phase factors.

The paper also presents an innovative formulation method in the context of the Wiener–Hopf technique for this class of problems. These equations are obtained directly in spectral domain subdividing the geometry of the problem into canonical sub-regions, and using the characteristic Greens' function procedure [39], the Mittag–Leffler's theorem [40,41] and a novel version of the Fredholm factorization, whose original version was introduced by these authors to solve Wiener–Hopf problems without closed-form solutions and reduces systematically an arbitrary Wiener–Hopf factorization problem to the Fredholm integral equation of the second kind [42,43], constituting a general-purpose factorization method. We here wish to clarify that we historically introduced the Fredholm factorization in [42,44] to get factorization of matrix WH kernels in impenetrable wedge diffraction problems. Due to the flexibility of the method, in subsequent works and applications we focused instead on the direct solution of WH problems in terms of WH unknowns by systematically reducing them to integral equations: the two applications of the method differ only in the source term. As a consequence, now, the original denomination 'Fredholm factorization' might be replaced with 'Fredholm decomposition'. However, these authors have been using the word 'factorization' since the origin of the method and different authors in literature now use the method more oriented to factorize matrices.

The novel version of the Fredholm factorization proposed in this paper is general and does not require any specialized (pre)factorization and solutions of systems of infinite equations for unknown coefficients (as in Jones' method). Indeed, when the Wiener–Hopf equations show incompleteness for the presence of sampled unknowns (in addition to classical WH unknowns), we apply a version of the integral Cauchy representation formula [9] that transforms the sampled unknowns into augmented kernel terms while applying the Fredholm factorization method, by preserving the properties of the Fredholm integral equation formulation. We demonstrate the key role of the Cauchy representations that are perfectly integrated into the Fredholm factorization method, in particular with entire functions. We note that this kind of representation closely relates our methodology to the Hilbert method and it has been inspired by [45], i.e. the contamination among methods allows once again progress in each other. Moreover, the explicitness of the integral equation formulation in terms of only physical spectral unknowns is a great advantage with respect to competing methods where a multi-step analysis of unknown coefficients is required for the convergence. A similar procedure already demonstrated efficacy in handling incomplete WH equations with non-entire unknowns, see [9]. Moreover, the Fredholm factorization is also the perfect instrument to consider exponential phase-factors as demonstrated for non-entire functions in [7].

The method proposed in this work yields a completed exact Wiener–Hopf modelling of the scattering problem and an exact representation of the solution in terms of Fredholm integral equations of the second kind, considering problems with both entire unknowns and exponential phase factors. Due to the convergence properties of Fredholm integral equation modelling of the problems (compact kernel), simple approximations like sample-and-hold yield high precision results via the reconstruction formula [46]. It is of major importance to note that the quality of a solution via the Fredholm factorization is also preserved for entire unknowns where pole singularities of remote sources do not guide the dominant behaviour of solutions. Finally, for a systematic application of the method, both Wiener–Hopf formulation and Fredholm integral equation modelling can be interpreted as network relations, to avoid redundancy.

To validate the method we investigate the particular but well-representative electromagnetic scattering problem of a slot in a thick metallic screen illuminated by plane-waves.

Different attempts to get solutions have been reported for this problem and for very similar ones such as the scattering by two sets of parallel plate waveguides with an hole and by parallel planes of finite length. Among the works that implement semi-analytical methods we recognize the application of the Wiener–Hopf technique in [16,19,21,27,32], of the mode-matching and coupled integral equations in [47–53], of Weber–Schafheitlin discontinuous integrals and Kobayashi–Nomura's method in [54,55], of combined modal expansion and ray tracing methods [56], and of Kirchhoff approximation and asymptotics [57,58] .

Unlike iterative methods as in Physical Optics (PO) and Ray Tracing (RT), the proposed technique describes the complete structure with an exact comprehensive mathematical model in the spectral domain avoiding multiple steps of interaction among separated structures, i.e. centres of scattering and diffraction. As a result, we obtain the true spectra of the field components, from which we extract by asymptotics physical/engineering phenomena excited by the structure, similar to what is achieved in closed-form analytical solutions.

The simplicity of the proposed reference validation test case (the thick slot) does not limit the applicability of the method in more complex problems where impenetrable/penetrable boundary conditions, finite dimension regions and localized sources are considered, see our preliminary work [10]. For what concerns the inclusion of impenetrable (impedance) boundary conditions, the method changes only for the enforcement of new constitutive relations among spectral field components, instead of cancelling them out from the equations as for perfect conducting boundaries. In the case of penetrable boundaries (penetrable regions of semi-infinite or finite dimensions) the number of subdomains is increased, yielding dedicated spectra equations with the imposition of continuity of the spectral field components. In general, the procedure continues as in the proposed validation test case, although equations became more numerous in the case of penetrable

regions and/or contain different spectral unknown field components according to impenetrable (impedance) boundary conditions. Finally, we comment on the case of localized source illumination. While the spectra of plane waves are constituted by poles defining standard/non-standard WH unknowns (see §2), the spectra of localized sources are functions depending on the physical branches of the problem. However, the WH formulation of the problem consists of the same steps, and it yields the same equations except for the source terms, thus the solution method is formally the same, although the more complicated source requires specific attention and computational resources while applying the Fredholm factorization.

This article is organized into eight sections. In §2, we introduce the geometry of the validation problem and the mathematical background in the spectral domain (Laplace transforms). Section 3 presents the Wiener–Hopf formulation of the problem according to the partition of the geometry in terms of modified and incomplete WH equations; the latter obtained by using a particular application of the characteristic Green's function procedure. Section 4 describes the procedure to render complete the incomplete equations, while the system of completed explicit Wiener–Hopf equations is reported in §5. The solution method based on the Fredholm factorization method and its extension is presented in §6 with a particular focus on completed Wiener–Hopf equations that requires the application of the Cauchy integral representation formula to get explicit Fredholm integral equations of the second kind. In §7, we show how to compute semi-analytical solutions in terms of spectral unknowns and how to estimate physical/engineering quantities by asymptotics from them in terms of geometrical theory of diffraction (GTD) field components and total far fields. The same section shows the validation and convergence of the proposed method in terms of spectra and physical quantities, also considering independent comparison with fully numerical solutions based on finite methods embedding singular modelling [59–62]. Finally, conclusions are reported in §8.

2. Description of the problem and mathematical statements

In order to enhance the understanding of the proposed methodology for the solution of Wiener–Hopf equations containing entire unknowns and exponential phase factors, we make reference to a practical electromagnetic scattering problem: the scattering of a plane wave by a slot in a thick perfectly electrically conducting (PEC) screen immersed in free space.

Figure 1 illustrates the problem where the slot is of thickness d and wideness s. In the following, we use reference coordinate systems with different origins. For the application of the Wiener–Hopf technique, we use Cartesian (x, y, z) and Cylindrical (ρ, φ, z) coordinate systems with origin O on the top-right corner of the left thick half-plane, while for the computation of diffraction and far-field by asymptotics we select as origins the centre of the slot on the top face A' with coordinates $(x, y, z) = (s/2, 0, z)$ and on the bottom face A'' with $(x, y, z) = (s/2, -d, z)$ respectively for fields in the top and in the bottom regions. Moreover, in the application of the Wiener–Hopf technique we also use the shifted Cartesian coordinate systems $(X = x - s, y, z)$ with origin O', although we privilege, as the main reference system, the one with origin O, if not otherwise specified.

Let us divide the problem, which is invariant along z, into three homogeneous regions (free space) of simple canonical shapes. Using the reference system selected for the Wiener–Hopf formulation with origin O, the half spaces $y > 0$ and $y < -d$ constitute respectively regions 1 and 2, while region 3 is the thick slot that occupies $0 < x < s$, $-d < y < 0$.

For the sake of simplicity, we study the problem at E_z polarization (the procedure can be duplicated for H_z polarization) with non-null field components $E_z(x, y), H_x(x, y), H_y(x, y)$ (invariant components to z, z dependence will be omitted from now) and we assume time harmonic fields with a time dependence specified $e^{+j\omega t}$, which is omitted. The problem is governed by Maxwell equations and in particular by the relevant Faraday's and Ampere's laws

$$\frac{\partial E_z}{\partial y} = -j\omega\mu_o H_x, \quad \frac{\partial E_z}{\partial x} = j\omega\mu_o H_y, \quad \frac{\partial H_y}{\partial x} - \frac{\partial H_x}{\partial y} = j\omega\epsilon_o E_z \tag{2.1}$$

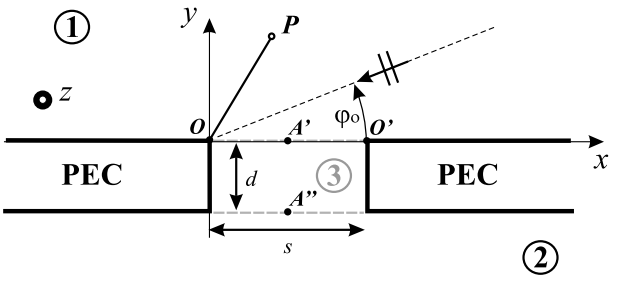

Figure 1. The scattering of a plane wave by a slot in a thick PEC screen immersed in free space. We define regions 1 and 2 respectively as the half spaces $y > 0$ and $y < -d$ and region 3 as the thick slot that occupies $0 < x < s$, $-d < y < 0$.

that yield the wave equation:

$$\frac{\partial^2 E_z}{\partial x^2} + \frac{\partial^2 E_z}{\partial y^2} + k^2 E_z = 0 \tag{2.2}$$

where $k = \omega\sqrt{\epsilon_o \mu_o}$ is the propagation constant of free space with the permittivity and permeability (ϵ_o, μ_o), also characterized by the free space impedance $Z_o = \sqrt{\mu_o/\epsilon_o}$.

With reference to figure 1, we impose PEC boundary conditions on the two thick half planes, i.e. $E_z = 0$ (PEC condition) for $(x = 0, s; -d < y < 0) \cup (x < 0; y = 0, -d) \cup (x > s; y = 0, -d)$. As the radial distance from the four edges $(x = 0, s; y = 0, -d)$ decrease to zero, E_z goes to zero as a polynomial with rational exponent (Meixner's edge condition [63,64]): for instance at point $O = (x = 0; y = 0)$ we have $E_z(\rho, \varphi) = O(\rho^{2/3})$. The radiation condition is enforced considering vanishing small losses in homogeneous medium, i.e. $k = k_r - jk_i$ $(k_r >> k_i > 0,\ k_i$ almost vanishing), thus $|E_z(\rho, \varphi) - E_z^g(\rho, \varphi)| < e^{-a\rho}$ (with $a > 0$), where E_z^g is the geometrical optics (GO) components of the total field E_z. The same assumption of small losses will be used for the correct definition of Wiener–Hopf unknowns. The uniqueness of the solution of the wave equation is therefore a consequence of the imposition of the boundary conditions, the edge condition, and the radiation conditions (for uniqueness theorem, see, for instance, [65,66]).

In the following, with reference to the origin O, we consider as a source of the problem an E_z plane wave normally incident on the structure with azimuthal incident direction $\varphi = \varphi_o$ from region 1:

$$E_z^i(\rho, \varphi) = E_o e^{jk\rho\cos(\varphi - \varphi_o)}, \quad H_x^i(\rho, \varphi) = -\frac{E_o}{Z_o}\sin(\varphi_o) e^{jk\rho\cos(\varphi - \varphi_o)}. \tag{2.3}$$

The formulation of the problem in the spectral domain is based on the definition of the following shifted right-unilateral, left-unilateral and right-finite Laplace transforms, respectively defined with different physical supports $(X > 0, y = 0, -d)$, $(x < 0, y = 0, -d)$, $(0 < x < s, y = 0, -d)$:

at $y = 0$

$$\begin{aligned} V_{1+}(\eta) &= \int_0^\infty \dot{E}_z(X, 0) e^{j\eta X} dX = e^{-j\eta s} \int_s^\infty E_z(x, 0) e^{j\eta x} dx, \\ I_{1+}(\eta) &= \int_0^\infty \dot{H}_x(X, 0) e^{j\eta X} dX = e^{-j\eta s} \int_s^\infty H_x(x, 0) e^{j\eta x} dx \end{aligned} \tag{2.4}$$

$$\begin{aligned} V_{1\pi+}(\eta) &= V_{1-}(-\eta) = \int_{-\infty}^0 E_z(x, 0) e^{-j\eta x} dx, \\ I_{1\pi+}(\eta) &= -I_{1-}(-\eta) = -\int_{-\infty}^0 H_x(x, 0) e^{-j\eta x} dx \end{aligned} \tag{2.5}$$

$$V_{1o}(\eta)=\int_0^s E_z(x,0)e^{j\eta x}dx,\qquad I_{1o}(\eta)=\int_0^s H_x(x,0)e^{j\eta x}dx \tag{2.6}$$

and at $y=-d$

$$V_{2+}(\eta)=\int_0^\infty \dot{E}_z(X,-d)e^{j\eta X}dX=e^{-j\eta s}\int_s^\infty E_z(x,-d)e^{j\eta x}dx,\qquad I_{2+}(\eta)=\int_0^\infty \dot{H}_x(X,-d)e^{j\eta X}dX=e^{-j\eta s}\int_s^\infty H_x(x,-d)e^{j\eta x}dx \tag{2.7}$$

$$V_{2\pi+}(\eta)=V_{2-}(-\eta)=\int_{-\infty}^0 E_z(x,-d)e^{-j\eta x}dx,\qquad I_{2\pi+}(\eta)=-I_{2-}(-\eta)=-\int_{-\infty}^0 H_x(x,-d)e^{-j\eta x}dx \tag{2.8}$$

$$V_{2o}(\eta)=\int_0^s E_z(x,-d)e^{j\eta x}dx,\qquad I_{2o}(\eta)=\int_0^s H_x(x,-d)e^{j\eta x}dx \tag{2.9}$$

with $\dot{E}_z(X,y)=E_z(x,y)$ and $\dot{H}_x(X,y)=H_x(x,y)$, recalling $X=x-s$. Moreover, due to the symmetric properties in WH formulations, we also use the auxiliary definitions of left-finite Laplace transforms

$$V_{1\pi o}(\eta)=e^{j\eta s}V_{1o}(-\eta),\ I_{1\pi o}(\eta)=e^{j\eta s}I_{1o}(-\eta),\ V_{2\pi o}(\eta)=e^{j\eta s}V_{2o}(-\eta),\ I_{2\pi o}(\eta)=e^{j\eta s}I_{2o}(-\eta) \tag{2.10}$$

which in explicit forms are defined for $y=0$

$$V_{1\pi o}(\eta)=\int_{-s}^0 E_z(X,0)e^{-j\eta X}dX=\int_0^s E_z(X,0)e^{-j\eta x}e^{j\eta s}dx=e^{j\eta s}V_{1o}(-\eta)$$
$$I_{1\pi o}(\eta)=\int_{-s}^0 H_x(X,0)e^{-j\eta X}dX=\int_0^s H_x(X,0)e^{-j\eta x}e^{j\eta s}dx=e^{j\eta s}I_{1o}(-\eta) \tag{2.11}$$

and similarly for $y=-d$

$$V_{2\pi o}(\eta)=\int_{-s}^0 E_z(X,-d)e^{-j\eta X}dX=\int_0^s E_z(X,-d)e^{-j\eta x}e^{j\eta s}dx=e^{j\eta s}V_{2o}(-\eta).$$
$$I_{2\pi o}(\eta)=\int_{-s}^0 H_x(X,-d)e^{-j\eta X}dX=\int_0^s H_x(X,-d)e^{-j\eta x}e^{j\eta s}dx=e^{j\eta s}I_{2o}(-\eta). \tag{2.12}$$

Note that, for our assumption, the π currents, representing left-unilateral Laplace transforms, are transformations of $-H_x$, while π currents, representing left-finite Laplace transforms, are transformations of $+H_x$.

The unilateral Laplace transforms (2.4), (2.5), (2.7), (2.8) labelled with (+) and (−) are respectively plus (+) and minus (−) functions in the Wiener–Hopf formulations, and in particular $V_{i\pi+}(\eta)$ and $I_{i\pi+}(\eta)$ $(i=1,2)$ are plus functions related to the minus functions $V_{i-}(\eta)$ and $I_{i-}(\eta)$. Plus (minus) functions are analytic functions that are regular in an upper (lower) half-plane $Im[\eta]>Im[\eta_{up}]$ $(Im[\eta]<Im[\eta_{lo}])$, go to zero at infinity as Laplace transforms and their integral definitions converge towards infinity $\eta\to+j\infty$ $(\eta\to-j\infty)$. The + (−) functions are non-standard (labelled ns), if $Im[\eta_{up}]>0$ $(Im[\eta_{lo}]<0)$, due to potential poles related to sources like plane waves. In fact, with plane wave illumination, only Geometrical Optics (GO) contributions generate pole

singularities of non-standard type. In particular, we note that the locations of singularities either GO or structural (in general such as surface and leaky wave poles due to media or surface impedance) are related to the x-direction of propagation. Considering an E_z plane wave incident with azimuthal direction $\varphi = \varphi_o$ (2.3), before imposing PEC boundary conditions, we obtain the corresponding plus right-unilateral Laplace transform (2.4)

$$V^i_{1+}(\eta) = e^{-j\eta s}\int_s^\infty E^i_z(x, y=0)e^{j\eta x}dx = \frac{jE_o e^{-j\eta_o s}}{\eta - \eta_o} \tag{2.13}$$

with a pole $\eta_o = -k\cos(\varphi_o)$ which lies in the 2nd or 4th quadrant of complex plane η along the segment that connects k to $-k$, according to our assumption of small vanishing losses. While $0 < \varphi_o < \pi/2$ ($\pi/2 < \varphi_o < \pi$), η_o is located in the 2nd (4th) quadrant, therefore $V^i_{1+}(\eta)$ is the non-standard (standard) plus function due to the regularity properties in the upper half-plane.

In general, each field component (GO, surface wave, leaky waves) is related to a singularity on the spectra that lies in the η complex plane, defining the regularity region of the spectral quantities. We note that poles on the spectra derive from the kernel singularities or field components with infinite geometrical support (since Laplace transforms of quantities with finite support yield entire functions). For example, with regard to GO components like reflected waves, we generalize (2.3) to

$$E^{go}_z(\rho, \varphi) = E_{go}e^{jk\rho\cos(\varphi - \varphi_{go})} \tag{2.14}$$

where φ_{go} (φ_{GO}) is the azimuthal direction of the wave with the lower case (upper case) subscripts go (GO) if referred to an incoming (outgoing) wave towards (from) the origin O of the reference system, thus $\varphi_{GO} = \varphi_{go} \pm \pi$. It yields that the spectrum of the plus right unilateral Laplace transform analogous to (2.13) of (2.14) contains a pole $\eta_{go} = -k\cos(\varphi_{go})$ whose location in the η complex plane depends on the angle φ_{go}. As non-standard poles are related only to sources (i.e. η_{go}), we notice that they are always located outside of the real axis, except in the limit punctual case of $\varphi_{go} = \pi/2$.

Equations (2.6), (2.9), (2.11), (2.12) report respectively right and left finite Laplace transforms which are entire functions (regular in the whole complex plane η) with an essential singularity behaviour of type $e^{j\eta s}$ and their integral definitions converge towards infinity $\eta \to +j\infty$. According to these properties, (2.6), (2.9), (2.11), (2.12) can be considered (+) plus-entire functions.

3. The Wiener–Hopf formulation

With reference to figure 1, we formulate the problem in spectral domain for the three regions (1, 2, 3), starting from the wave equation (2.2) with the application of the Laplace transforms (2.4)–(2.12) and, the mathematical statements relative to the constitutive relations, the radiation condition and the boundary conditions reported in §2.

(a) Regions 1 and 2: the homogeneous half spaces

In the homogeneous half spaces, region 1 ($y > 0$) and region 2 ($y < -d$) of figure 1, we apply the bilateral Laplace transforms along x (3.1) to non-null field transverse-to-y components

$$\begin{aligned} v(\eta, y) &= \int_{-\infty}^{\infty} E_z(x, y)e^{j\eta x}dx \\ i(\eta, y) &= \int_{-\infty}^{\infty} H_x(x, y)e^{j\eta x}dx \end{aligned} \tag{3.1}$$

to represent Maxwell's equation (2.1) in the spectral domain. It yields the following equivalent spectral transmission line equation modelling, as commonly reported in literature for the spectral representation of planar stratified regions, see for instance [4,7,67] and references therein:

$$\begin{aligned} -\frac{dv(\eta,y)}{dy} &= j\xi(\eta)Z_c(\eta)i(\eta,y) \\ -\frac{di(\eta,y)}{dy} &= j\xi(\eta)Y_c(\eta)v(\eta,y) \end{aligned} \tag{3.2}$$

where

$$\xi = \xi(\eta) = \sqrt{k^2 - \eta^2} \tag{3.3}$$

is the spectral propagation constant and

$$Z_c = Z_c(\eta) = 1/Y_c = 1/Y_c(\eta) = kZ_o/\xi \tag{3.4}$$

is the spectral characteristic impedance of the transmission line (TL) along y. Since $\xi(\eta)$ is a multi-valued function of η, in the following, we assume as a proper sheet of $\xi(\eta)$ the one with $\xi(0) = k$ and as branch lines the lines $Im[\xi(\eta)] = 0$ (Ch. 5.3b of [67]) or the vertical lines ($Re[\eta] = Re[k]$, $Im[\eta] < Im[k]$) and ($Re[\eta] = Re[-k]$, $Im[\eta] > Im[-k]$).

For the region 1 ($y > 0$) and the region 2 ($y < -d$), we obtain from the spectral transmission line representation the following admittance one-port models

$$\begin{aligned} i(\eta,0) &= Y_c(\eta)\, v(\eta,0) \\ i(\eta,-d) &= -Y_c(\eta)\, v(\eta,-d) \end{aligned} \tag{3.5}$$

that can be expressed in terms of the Laplace transforms defined in (2.4)–(2.12) for the WH formulation:

$$\begin{aligned} -I_{1\pi+}(-\eta) + I_{1o}(\eta) + e^{j\eta s}I_{1+}(\eta) &= Y_c(\eta)[V_{1\pi+}(-\eta) + V_{1o}(\eta) + e^{j\eta s}V_{1+}(\eta)], \\ I_{2\pi+}(-\eta) - I_{2o}(\eta) - e^{j\eta s}I_{2+}(\eta) &= Y_c(\eta)[V_{2\pi+}(-\eta) + V_{2o}(\eta) + e^{j\eta s}V_{2+}(\eta)]. \end{aligned} \tag{3.6}$$

The system of WH equations for regions 1 and 2 is obtained after imposing the boundary conditions, i.e. $E_z = 0$ (PEC condition) for $(x = 0, s; -d < y < 0) \cup (x < 0; y = 0, -d) \cup (x > s; y = 0, -d)$, it yields from (3.6) respectively :

$$-I_{1\pi+}(-\eta) + I_{1o}(\eta) + e^{j\eta s}I_{1+}(\eta) = Y_c(\eta)V_{1o}(\eta) \tag{3.7}$$

$$I_{2\pi+}(-\eta) - I_{2o}(\eta) - e^{j\eta s}I_{2+}(\eta) = Y_c(\eta)V_{2o}(\eta). \tag{3.8}$$

Both (3.7) and (3.8) are explicit WH equations that can be interpreted as one port network model. Moreover, they are in substance longitudinally modified WH equations for the presence of plus entire functions in addition to plus and minus ones and exponential phase factors. As stated in the introduction, see §1, these equations were introduced and studied by Jones through an ad-hoc popular method that exploits the analytical properties of the WH unknowns.

Alternatively, this class of equations (that contains three unknowns) can be studied exploiting the analytical properties of the WH unknowns and using suitable algebraic manipulations on themselves. In particular, by substituting η with $-\eta$, and by multiplying by $e^{j\eta s}$ the scalar modified equation (3.7), we obtain four non-redundant WH equations (see first block in (5.1)). These four equations can be reduced to classical matrix WH equations amenable to classical and/or Fredholm factorization [4]. The procedure can be repeated for the scalar modified equation (3.8) linked to the four equations of the second block in (5.1).

(b) Region 3: the homogeneous thick slot

To model the homogeneous thick slot region 3 ($0 < x < s$, $-d < y < 0$) of figure 1, we apply the right-finite Laplace transform along x (2.6), (2.9) to $E_z(x,y), H_x(x,y)$ field components

$$\tilde{E}_z(\eta,y) = \int_0^s E_z(x,y)e^{j\eta x}dx, \quad \tilde{H}_x(\eta,y) = \int_0^s H_x(x,y)e^{j\eta x}dx \tag{3.9}$$

to represent the wave equation (2.2) in the spectral domain. It yields:

$$\left(\frac{d^2}{dy^2} + \xi^2(\eta)\right)\tilde{E}_z(\eta,y) = f(\eta,y) \tag{3.10}$$

with ξ defined in (3.3) and where

$$f(\eta,y) = j\eta[E_z(s_-,y)e^{j\eta s} - E_z(0_+,y)] - \frac{\partial}{\partial x}[E_z(s_-,y)]e^{j\eta s} + \frac{\partial}{\partial x}[E_z(0_+,y)] \tag{3.11}$$

due to the properties of right-finite Laplace transform on derivatives. The application of Maxwell's equation (2.1) and of PEC boundary conditions $E_z = 0$ (PEC condition) for $(x = 0, s; -d < y < 0)$ yields

$$f(\eta,y) = -j\omega\mu_o H_y(s_-,y)e^{j\eta s} + j\omega\mu_o H_y(0_+,y). \tag{3.12}$$

Equation (3.10) is an ordinary differential equation of second order in y that holds for $-d < y < 0$ with the forcing function $f_\eta(\eta,y)$ and the boundary conditions of continuity at $y = 0, -d$ in the spectral domain:

$$\begin{aligned} &\tilde{E}_z(\eta,0_+) = \tilde{E}_z(\eta,0_-) = V_{1o}(\eta), \quad \tilde{H}_x(\eta,0_+) = \tilde{H}_x(\eta,0_-) = I_{1o}(\eta) \\ &\tilde{E}_z(\eta,d_+) = \tilde{E}_z(\eta,d_-) = V_{2o}(\eta), \quad \tilde{H}_x(\eta,d_+) = \tilde{H}_x(\eta,d_-) = I_{2o}(\eta) \end{aligned} \tag{3.13}$$

with reference to the definitions (2.6), (2.9), and (3.9).

In classical literature, the solution of this type of differential problem can be expressed as the sum of a particular integral and a linear combination of homogeneous solutions. We follow the procedure outlined in [39] where the characteristic Green's function method for the definition of the particular integral is generalized and applied to problems with unmixed non-homogeneous boundary conditions, by building the Green's function in terms of arbitrary homogeneous solutions (ignoring initially the boundary conditions of the problem). The Green's function must fulfil three essential conditions: (i) it must be continuous at $y = y'$ with y observation point and y' integration variable in the particular integral, (ii) it must have a derivative with jump at $y = y'$, and (iii) it must be solution of the corresponding homogeneous differential equations.

Consequently, the solution of a differential problem with the forcing term and the boundary conditions is constituted by the combination of the particular integral and the homogeneous component of the solution, with the arbitrary coefficients uniquely determined by the application of the boundary conditions.

Without loss of generality, to build a Green's function for the problem (3.10), we here select from the set of homogeneous solutions

$$\begin{cases} \overleftarrow{\varphi}_\eta(y) = \sin[(\xi)(y+d)] \\ \vec{\varphi}_\eta(y) = \sin(\xi y) \end{cases} \tag{3.14}$$

which satisfy PEC boundary conditions respectively at $y = -d, 0$, i.e. they are null at $y = -d, 0$. As we notice, this selection is not directly related to the physics of the problem (there is no PEC interface at $y = -d, 0$), however the construction of the Green's function for the particular integral

together with the selection of coefficients on the homogeneous part of the solution will be enforced in such a way as to satisfy the physical boundary conditions of continuity at $y=-d,0$ (3.13).

According to [39] and (3.14), the Green's function is

$$g_\eta(y,y') = \frac{\overleftarrow{\varphi}_\eta(y_<)\,\vec{\varphi}_\eta(y_>)}{W_r\left[\overleftarrow{\varphi}_\eta(y_<),\vec{\varphi}_\eta(y_>)\right]} = \frac{\sin(\xi y_>)\sin\left(\xi\left(y_<+d\right)\right)}{\xi\sin(\xi d)} \tag{3.15}$$

where $W_r\left[\overleftarrow{\varphi}_{1\eta}(y),\vec{\varphi}_{1\eta}(y)\right]$ is the Wronskian of the two functions $\overleftarrow{\varphi}_\eta(y)$ and $\vec{\varphi}_\eta(y)$ and $y_<$ and $y_>$ denote respectively the lesser and the greater of quantities y and y'. The solution of (3.10) with continuity boundary conditions at $y=-d,0$ (unmixed non-homogeneous boundary conditions) is therefore

$$\tilde{E}_{z+}(\eta,y) = \int_{-d}^{0} g_\eta(y,y')f(\eta,y')\,dy' + A_1(\eta)\overleftarrow{\varphi}_\eta(y) + A_2(\eta)\vec{\varphi}_\eta(y) \tag{3.16}$$

with arbitrary coefficients $A_1(\eta)$ and $A_2(\eta)$.

Because of the continuity boundary conditions at $y=-d,0$ (3.13), we now establish the relationship among the arbitrary coefficients $A_1(\eta)$ and $A_2(\eta)$ and the spectral fields at the interfaces (2.6), (2.9), i.e.

$$\begin{aligned}\tilde{E}_{z+}(\eta,0) &= V_{1o}(\eta) = +A_1(\eta,)\sin(\xi d)\\ \tilde{E}_{z+}(\eta,-d) &= V_{2o}(\eta) = -A_2(\eta)\sin(\xi d)\end{aligned} \tag{3.17}$$

thus

$$A_1(\eta) = \frac{V_{1o}(\eta)}{\sin(\xi d)},\quad A_2(\eta) = -\frac{V_{2o}(\eta)}{\sin(\xi d)}. \tag{3.18}$$

The imposition of the second condition of continuity (3.13), i.e. on the H_x component, yields the WH formulation of region 3 in terms of the spectral fields at the interfaces (2.6), (2.9). In fact, taking into consideration the first of Maxwell's equations reported in (2.1) with $\tilde{E}_{z+}(\eta,y)$ defined in (3.16) with (3.18) and the continuity relations (3.13) for H_x, we get the following two equations that respectively hold at $y=0,-d$

$$\begin{aligned}I_{1o}(\eta) &= -Y_{11}(\eta)V_{1o}(\eta) - Y_{12}(\eta)V_{2o}(\eta) + \frac{\int_{-d}^{0}\sin\left[\xi(y'+d)\right]f(\eta,y')dy}{-jkZ_o\sin(\xi d)}\\ I_{2o}(\eta) &= Y_{21}(\eta)V_{1o}(\eta) + Y_{22}(\eta)V_{2o}(\eta) + \frac{\int_{-d}^{0}\sin(\xi y')f(\eta,y')dy}{-jkZ_o\sin(\xi d)}\end{aligned} \tag{3.19}$$

with

$$Y_{11}(\eta) = Y_{22}(\eta) = -jY_c(\eta)\cot(\xi d),\quad Y_{12}(\eta) = Y_{21}(\eta) = jY_c(\eta)\csc(\xi d) \tag{3.20}$$

and $Y_c(\eta)$ and $f(\eta,y')$ defined respectively in (3.4) and (3.12).

Since the integral part in (3.19) is not explicit in terms of the spectral unknowns, the equations are considered incomplete (not explicit) WH equations, however (3.19) can be interpreted as a two port network model of the thick slot, closely resembling the two port network model of an infinite layer of thickness d except for the presence of the particular integral terms that can be considered as local dependent sources.

4. Solving incompleteness of Wiener–Hopf equations: region 3

Unlike what happens in regions 1 and 2, where we have obtained modified Wiener–Hopf equations, the finiteness of the section's shape of region 3 yields incomplete WH equations as reported

in §3b at (3.19). We exploit the Mittag–Leffler theorem [40,41] to solve incompleteness, by representing the particular integrals via samples of the physical spectral unknowns in η at physical poles of the problems. We notice, alternatively to [14], that the sampling is related to the structure of particular integrals and specifically to their denominators.

With reference to (3.19), we notice that the denominators of the integral terms are defined in terms of $\sin(\xi d)$ that provides the poles

$$\xi_n = n\pi/d, \quad \eta_n = \sqrt{k^2 - \left(\frac{n\pi}{d}\right)^2}, \quad n \in \mathbb{N}_0 \tag{4.1}$$

which are the same poles of the admittances $Y_{ij}(\eta)$ (η) (3.20). Notice that the poles (4.1) are also those of a parallel plate waveguide of width d (i.e. modal propagation constants along y), thus with a physical meaning, at least in terms of the equivalence theorem [66].

We observe that the integrals in (3.19) can be written as

$$\begin{aligned} \frac{\int_{-d}^{0} \sin[\xi(y'+d)] f(\eta,y')dy'}{-jkZ_o \sin(\xi d)} &= -e^{j\eta s} q_o(\eta) + p_o(\eta) \\ \frac{\int_{-d}^{0} \sin(\xi y') f(\eta,y')dy'}{-jkZ_o \sin(\xi d)} &= -e^{j\eta s} s_o(\eta) + r_o(\eta) \end{aligned} \tag{4.2}$$

where, considering (3.12), we obtain the explicit expressions at the second members of (4.3)

$$\begin{aligned} p_o(\eta) &= \frac{\int_{-d}^{0} \sin(\xi(y'+d))(jkZ_o)H_y(0_+,y')dy'}{-jkZ_o \sin(\xi d)} = \sum_{n=1}^{\infty} \frac{A_n}{\xi^2-\xi_n^2} = -\sum_{n=1}^{\infty} \frac{A_n}{\eta^2-\eta_n^2}. \\ q_o(\eta) &= \frac{\int_{-d}^{0} \sin(\xi(y'+d))(jkZ_o)H_y(s_-,y')dy'}{-jkZ_o \sin(\xi d)} = \sum_{n=1}^{\infty} \frac{C_n}{\xi^2-\xi_n^2} = -\sum_{n=1}^{\infty} \frac{C_n}{\eta^2-\eta_n^2}. \\ r_o(\eta) &= \frac{\int_{-d}^{0} \sin(\xi y')(jkZ_o)H_y(0_+,y')dy'}{-jkZ_o \sin(\xi d)} = \sum_{n=1}^{\infty} \frac{B_n}{\xi^2-\xi_n^2} = -\sum_{n=1}^{\infty} \frac{B_n}{\eta^2-\eta_n^2}. \\ s_o(\eta) &= \frac{\int_{-d}^{0} \sin(\xi y')(jkZ_o)H_y(s_-,y')dy'}{-jkZ_o \sin(\xi d)} = \sum_{n=1}^{\infty} \frac{D_n}{\xi^2-\xi_n^2} = -\sum_{n=1}^{\infty} \frac{D_n}{\eta^2-\eta_n^2}. \end{aligned} \tag{4.3}$$

We notice that the second members of (4.3) are even meromorphic functions of ξ, for which the application of the Mittag–Leffler theorem [40,41] provides the representations reported at the third members of (4.3) with coefficients A_n, B_n, C_n, D_n to be determined. Observing the new representation of WH equation (3.19) of region 3 after substituting (4.2) and (4.3)

$$\begin{aligned} -e^{j\eta s} q_o(\eta) + p_o(\eta) - I_{1o}(\eta) &= Y_{11}(\eta)V_{1o}(\eta) + Y_{12}(\eta)V_{2o}(\eta) \\ -e^{j\eta s} s_o(\eta) + r_o(\eta) - I_{2o}(\eta) &= -Y_{21}(\eta)V_{1o}(\eta) - Y_{22}(\eta)V_{2o}(\eta) \end{aligned} \tag{4.4}$$

we notice that, while $p_o(\eta), q_o(\eta), r_o(\eta), s_o(\eta)$ and the admittances $Y_{ij}(\eta)$ (η) (3.20) have poles at $\eta = \pm\eta_n$, the entire spectral unknowns $V_{1o}(\eta), I_{1o}(\eta), V_{2o}(\eta), I_{2o}(\eta)$ are regular functions in the whole complex plane η. Consequently, we can derive expressions for A_n, B_n, C_n, D_n in $p_o(\eta), q_o(\eta), r_o(\eta), s_o(\eta)$ by imposing the balance of the poles $\eta = \pm\eta_n$ in the above equation (4.4).

Going back to the definition of $V_{1o}(\eta), I_{1o}(\eta), V_{2o}(\eta), I_{2o}(\eta)$ (2.6), (2.9), we recall that the right-finite Laplace transform integrals converge for $\eta \to +j\infty$ but diverge for $\eta \to -j\infty$, therefore the sampling on entire unknowns becomes unstable for $+\eta_n$ (4.1) with growing n. To avoid this issue, while implementing the estimation of A_n, B_n, C_n, D_n, we resort to the symmetry property of WH equations and the definition of the π auxiliary entire unknowns $V_{1\pi o}(\eta), I_{1\pi o}(\eta), V_{2\pi o}(\eta), I_{2\pi o}(\eta)$

(2.10), whose transform integrals converge for $\eta \to +j\infty$ and diverge for $\eta \to -j\infty$. This yields a different sets of equations derived from (4.4):

$$\begin{aligned} -q_o(\eta) + e^{j\eta s} p_o(\eta) - I_{1\pi o}(\eta) &= Y_{11}(\eta) V_{1\pi o}(\eta) + Y_{12}(\eta) V_{2\pi o}(\eta). \\ -s_o(\eta) + e^{j\eta s} r_o(\eta) - I_{2\pi o}(\eta) &= -Y_{21}(\eta) V_{1\pi o}(\eta) - Y_{22}(\eta) V_{2\pi o}(\eta). \end{aligned} \tag{4.5}$$

We now have four equations (4.4) and (4.5) that allow the determination of A_n, B_n, C_n, D_n just sampling at $\eta = -\eta_n$, where all the unknowns also converge for increasing values of n. In order to implement the system of equations, when we preliminary estimate the residues of $p_o(\eta), q_o(\eta), r_o(\eta), s_o(\eta)$ (4.3) and $Y_{ij}(\eta)$ (3.20) at $\eta = -\eta_n$, we get:

$$\begin{aligned} &\mathrm{Res}[p_o(\eta), -\eta_n] = \frac{A_n}{2\xi_n}, \quad \mathrm{Res}[q_o(\eta), -\eta_n] = \frac{C_n}{2\xi_n}. \\ &\mathrm{Res}[r_o(\eta), -\eta_n] \frac{B_n}{2\xi_n}, \quad \mathrm{Res}[s_o(\eta), -\eta_n] = \frac{D_n}{2\xi_n}. \\ &\mathrm{Res}[Y_{11}(\eta), -\eta_n] = \mathrm{Res}[Y_{22}(\eta), -\eta_n] = -\frac{jn^2\pi^2}{d^3 k Z_o \xi_n}. \\ &\mathrm{Res}[Y_{12}(\eta), -\eta_n] = \mathrm{Res}[Y_{21}(\eta), -\eta_n] = \frac{jn^2\pi^2(-1)^n}{d^3 k Z_o \xi_n}. \end{aligned} \tag{4.6}$$

Imposing the balance on the poles in (4.4) and (4.5), we get the system of equations for each $n \in \mathbb{N}_0$

$$\begin{aligned} -e^{-j\eta_n s}\frac{C_n}{2\eta_n} + \frac{A_n}{2\eta_n} &= -\frac{j(\pi n)^2}{d^3 k Z_o \eta_n} V_{1o}(-\eta_n) + \frac{j(\pi n)^2(-1)^n}{d^3 k Z_o \eta_n} V_{2o}(-\eta_n) \\ -\frac{C_n}{2\eta_n} + e^{-j\eta_n s}\frac{A_n}{2\eta_n} &= -\frac{j(\pi n)^2}{d^3 k Z_o \eta_n} V_{1\pi o}(-\eta_n) + \frac{j(\pi n)^2(-1)^n}{d^3 k Z_o \eta_n} V_{2\pi o}(-\eta_n) \\ -e^{-j\eta_n s}\frac{D_n}{2\eta_n} + \frac{B_n}{2\eta_n} &= -\frac{j(\pi n)^2(-1)^n}{d^3 k Z_o \eta_n} V_{1o}(-\eta_n) + \frac{j(\pi n)^2}{d^3 k Z_o \eta_n} V_{2o}(-\eta_n) \\ -\frac{D_n}{2\eta_n} + e^{-j\eta_n s}\frac{B_n}{2\eta_n} &= -\frac{j(\pi n)^2(-1)^n}{d^3 k Z_o \eta_n} V_{1\pi o}(-\eta_n) + \frac{j(\pi n)^2}{d^3 k Z_o \eta_n} V_{2\pi o}(-\eta_n) \end{aligned} \tag{4.7}$$

whose solution provides

$$\begin{aligned} A_n &= -\frac{2j\pi^2 n^2 e^{j\eta_n s}\left[e^{j\eta_n s} V_{1o}(-\eta_n) - (-1)^n e^{j\eta_n s} V_{2o}(-\eta_n) - V_{1\pi o}(-\eta_n) + (-1)^n V_{2\pi o}(-\eta_n)\right]}{d^3 k Z_o \left(-1 + e^{j2\eta_n s}\right)}. \\ C_n &= -\frac{2j\pi^2 n^2 e^{j\eta_n s}\left[V_{1o}(-\eta_n) - (-1)^n V_{2o}(-\eta_n) - e^{j\eta_n s} V_{1\pi o}(-\eta_n) + (-1)^n e^{j\eta_n s} V_{2\pi o}(-\eta_n)\right]}{d^3 k Z_o \left(-1 + e^{j2\eta_n s}\right)}. \\ B_n &= (-1)^n A_n, \quad D_n = (-1)^n C_n. \end{aligned} \tag{4.8}$$

Now, the system of the WH equations (4.4) and (4.5) with (4.3) and (4.8) constitutes an explicit (completed) set of WH equations in terms of the spectral unknowns in continuous and sampled forms.

5. Explicit set of Wiener–Hopf equations for the thick slot problem

To solve in a stable manner the incompleteness of equation (4.4) for region 3, in §4 we used the symmetric equation (4.5). To formalize a set of non-redundant equations for the entire problem of figure 1, we also recover the explicit modified WH equations of regions 1 and 2 reported at (3.7), (3.8) and we symmetrize and duplicate them substituting η with $-\eta$, by multiplying them by $e^{j\eta s}$,

using the definition of $V_{1\pi o}(\eta), I_{1\pi o}(\eta), V_{2\pi o}(\eta), I_{2\pi o}(\eta)$ (2.10). The final set of WH equations that we consider is:

$$\begin{cases} \begin{cases} -I_{1\pi+}(-\eta)+I_{1o}(\eta)+e^{j\eta s}I_{1+}(\eta)=Y_c(\eta)V_{1o}(\eta) \\ -I_{1\pi+}(\eta)+I_{1o}(-\eta)+e^{-j\eta s}I_{1+}(-\eta)=Y_c(\eta)V_{1o}(-\eta) \\ -e^{j\eta s}I_{1\pi+}(\eta)+I_{1\pi o}(\eta)+I_{1+}(-\eta)=Y_c(\eta)V_{1\pi o}(\eta) \\ -e^{-j\eta s}I_{1\pi+}(-\eta)+I_{1\pi o}(-\eta)+I_{1+}(\eta)=Y_c(\eta)V_{1\pi o}(-\eta) \end{cases} \\ \begin{cases} I_{2\pi+}(-\eta)-I_{2o}(\eta)-e^{j\eta s}I_{2+}(\eta)=Y_c(\eta)V_{2o}(\eta) \\ I_{2\pi+}(\eta)-I_{2o}(-\eta)-e^{-j\eta s}I_{2+}(-\eta)=Y_c(\eta)V_{2o}(-\eta) \\ e^{j\eta s}I_{2\pi+}(\eta)-I_{2\pi o}(\eta)-I_{2+}(-\eta)=Y_c(\eta)V_{2\pi o}(\eta) \\ e^{-j\eta s}I_{2\pi+}(-\eta)-I_{2\pi o}(-\eta)-I_{2+}(\eta)=Y_c(\eta)V_{2\pi o}(-\eta) \end{cases} \\ \begin{cases} -I_{s1o}(\eta)-I_{1o}(\eta)=Y_{11}(\eta)V_{1o}(\eta)+Y_{12}(\eta)V_{2o}(\eta) \\ I_{s2o}(\eta)+I_{2o}(\eta)=Y_{21}(\eta)V_{1o}(\eta)+Y_{22}(\eta)V_{2o}(\eta) \\ -I_{s1\pi o}(\eta)-I_{1\pi o}(\eta)=Y_{11}(\eta)V_{1\pi o}(\eta)+Y_{12}(\eta)V_{2\pi o}(\eta) \\ I_{s2\pi o}(\eta)+I_{2\pi o}(\eta)=Y_{21}(\eta)V_{1\pi o}(\eta)+Y_{22}(\eta)V_{2\pi o}(\eta) \end{cases} \end{cases} \tag{5.1}$$

with

$$\begin{aligned} -I_{s1o}(\eta)&=-e^{j\eta s}q_o(\eta)+p_o(\eta)=-\sum_{n=1}^{\infty}\frac{A_n}{\eta^2-\eta_n^2}+e^{j\eta s}\sum_{n=1}^{\infty}\frac{C_n}{\eta^2-\eta_n^2} \\ -I_{s2o}(\eta)&=-e^{j\eta s}s_o(\eta)+r_o(\eta)=-\sum_{n=1}^{\infty}\frac{B_n}{\eta^2-\eta_n^2}+e^{j\eta s}\sum_{n=1}^{\infty}\frac{D_n}{\eta^2-\eta_n^2} \\ -I_{s1\pi o}(\eta)&=-q_o(\eta)+e^{j\eta s}p_o(\eta)=-e^{j\eta s}\sum_{n=1}^{\infty}\frac{A_n}{\eta^2-\eta_n^2}+\sum_{n=1}^{\infty}\frac{C_n}{\eta^2-\eta_n^2} \\ -I_{s2\pi o}(\eta)&=-s_o(\eta)+e^{j\eta s}r_o(\eta)=-e^{j\eta s}\sum_{n=1}^{\infty}\frac{B_n}{\eta^2-\eta_n^2}+\sum_{n=1}^{\infty}\frac{D_n}{\eta^2-\eta_n^2} \end{aligned} \tag{5.2}$$

and where A_n, B_n, C_n, D_n are reported in terms of spectral samples at (4.8), thus

$$\begin{aligned} I_{s1o}(\eta)&=\sum_{n=1}^{\infty}\left[h_{11}(\eta,n)V_{1o}(-\eta_n)+h_{12}(\eta,n)V_{2o}(-\eta_n)+h_{13}(\eta,n)V_{1\pi o}(-\eta_n)+h_{14}(\eta,n)V_{2\pi o}(-\eta_n)\right] \\ I_{s2o}(\eta)&=-\sum_{n=1}^{\infty}\left[h_{21}(\eta,n)V_{1o}(-\eta_n)+h_{22}(\eta,n)V_{2o}(-\eta_n)+h_{23}(\eta,n)V_{1\pi o}(-\eta_n)+h_{24}(\eta,n)V_{2\pi o}(-\eta_n)\right] \\ I_{s1\pi o}(\eta)&=\sum_{n=1}^{\infty}\left[h_{31}(\eta,n)V_{1o}(-\eta_n)+h_{32}(\eta,n)V_{2o}(-\eta_n)+h_{33}(\eta,n)V_{1\pi o}(-\eta_n)+h_{34}(\eta,n)V_{2\pi o}(-\eta_n)\right] \\ I_{s2\pi o}(\eta)&=-\sum_{n=1}^{\infty}\left[h_{41}(\eta,n)V_{1o}(-\eta_n)+h_{42}(\eta,n)V_{2o}(-\eta_n)+h_{43}(\eta,n)V_{1\pi o}(-\eta_n)+h_{44}(\eta,n)V_{2\pi o}(-\eta_n)\right] \end{aligned} \tag{5.3}$$

where we omit to report the explicit expressions of $h_{ij}(\eta, n)$.

Notice that the first, the second and the third blocks of the explicit WH equation (5.1) respectively model regions 1, 2, 3. We note that (5.1) are homogeneous WH equations even in the presence of plane wave illuminations as the source terms are implicitly stored in the not-entire WH unknowns, see p. 183 of [4].

The set of equation (5.1) might be erroneously considered redundant because in each block from one equation we get the other three after mathematical manipulations; on the contrary, the regularity properties of the WH unknowns in the set of equation (5.1) are fundamental to get stable convergent solutions through a generalized form of the Fredholm factorization, reported in the next section.

6. Fredholm factorization for classical and completed equations

In the application of the Fredholm factorization to classical WH equations, we use the additive decomposition of an arbitrary analytic function into plus and minus components, i.e. $F(\eta) = F_+(\eta) + F_-(\eta)$, by means of the Cauchy decomposition formula [1,42]:

$$\begin{aligned} F_+(\eta) &= \frac{1}{2\pi j}\int_{\gamma_1}\frac{F(\eta')}{\eta'-\eta}d\eta' = \frac{1}{2}F(\eta) + \frac{PV}{2\pi j}\int_{-\infty}^{+\infty}\frac{F(\eta')}{\eta'-\eta}d\eta, \quad \eta\in\mathbb{R} \\ F_-(\eta) &= -\frac{1}{2\pi j}\int_{\gamma_2}\frac{F(\eta')}{\eta'-\eta}d\eta' = \frac{1}{2}F(\eta) - \frac{PV}{2\pi j}\int_{-\infty}^{+\infty}\frac{F(\eta')}{\eta'-\eta}d\eta', \quad \eta\in\mathbb{R} \end{aligned} \tag{6.1}$$

where PV denotes the principal value and γ_1 and γ_2 are, respectively, the *smile* and the *frown* integration lines in the η-plane [14,42], i.e. the real axis of the η'-plane indented at $\eta' = \eta$ with a small semi-circumference respectively in the lower and in the upper half plane.

In the next sub-sections, we extensively apply the following generalized Cauchy decomposition formula [4,42] in the presence of potential non-standard singularities (offending singularities in the regularity half-plane as defined in §2):

$$\begin{aligned} &\frac{1}{2\pi j}\int_{\gamma_1}\frac{F_+(\eta')}{\eta'-\eta}d\eta' = F_+(\eta) - F_+^{ns}(\eta), \quad \frac{1}{2\pi j}\int_{\gamma_2}\frac{F_+(\eta')}{\eta'-\eta}d\eta' = -F_+^{ns}(\eta) \\ &\frac{1}{2\pi j}\int_{\gamma_2}\frac{F_-(\eta')}{\eta'-\eta}d\eta' = -F_-(\eta) + F_-^{ns}(\eta), \quad \frac{1}{2\pi j}\int_{\gamma_1}\frac{F_-(\eta')}{\eta'-\eta}d\eta' = F_-^{ns}(\eta) \end{aligned} \tag{6.2}$$

for $\eta\in\mathbb{R}$ and, where $F_\pm^{ns}(\eta)$ are non-standard parts of $F_\pm(\eta)$, i.e. $F_\pm(\eta) = F_\pm^{s}(\eta) + F_\pm^{ns}(\eta)$ with $F_\pm^{s}(\eta)$ being the standard parts. From a computational point of view the non-standard parts are Laplace transforms related to GO components as defined in §2, see (2.13) and (2.14), and therefore they can be easily estimated by GO. We also note that (6.1) and (6.2) can be extended to finite Laplace transforms, considering the property of being entire functions.

The Fredholm factorization method [4,42,43] is founded on the decomposition formula (6.2) and it reduces the system of spectral WH equations to integral representations of the second kind with compact kernels, by eliminating one kind of unknown (plus or minus). In the following, we privilege the elimination of the minus unknowns for the solution of WH equations.

In this work, we generalize the application of the Fredholm factorization to entire unknowns and to completed equations, where the original incompleteness of equations has been treated by means of the Mittag–Leffler theorem [40,41]. Making reference to the proposed reference example (figure 1), we have obtained the sets of explicit equations reported in §5, whose explicitness is defined in terms of samples of the spectral entire unknowns at physical poles. We note that this formulation, although explicit and physically related, requires the determination of infinite samples that apparently resumes the drawbacks of alternative techniques reported in §1.

Alternatively, in this work, we formulate the solution using a generalized form of the Fredholm factorization that yields explicit Fredholm integral equations of the second kind, removing the requirements for solving infinite coefficients, and is amenable to simple approximations for high precision results [46]. The method is general and does not require any specialized (pre)factorization and solutions of systems of infinite equations for unknown coefficients.

The completeness solved via the Mittag–Leffler theorem is here combined with a special version of the integral Cauchy representation formula. The consequent application of the Fredholm factorization to the whole problem yields explicit Fredholm integral equation formulations for the solution of the WH problem with augmented kernels due to Cauchy's formula terms, preserving convergence properties. In particular, we observe that the method allows us to get regularized integral representations with compact kernels.

(a) Application to classical WH equations: regions 1 and 2

In regions 1 and 2, explicit modified WH equations hold, i.e. the first two blocks in (5.1). The apparently redundant equations in the blocks are here exploited to get symmetric Fredholm integral equations via the classical application of the Fredholm factorization for a formulation just in terms of plus unknowns, i.e. by eliminating the minus ones. In the following, we assume that the non-standard parts of the WH unknowns are related to a plane wave source characterized by the pole η_o (2.13).

Let us focus the application of the Fredholm factorization on the first two equations of (5.1) and subsequently we repeat the procedure for the other six equations. Considering the first of (5.1)

$$-I_{1\pi+}(-\eta) + I_{1o}(\eta) + e^{j\eta s} I_{1+}(\eta) = Y_c(\eta) V_{1o}(\eta) \tag{6.3}$$

the application of the smile contour γ_1 integration (6.2) to the left hand side (LHS) of (6.3) yields

$$\frac{1}{2\pi j}\int_{\gamma_1} \frac{-I_{1\pi+}(-\eta') + I_{1o}(\eta') + e^{j\eta' s} I_{1+}(\eta')}{\eta' - \eta} d\eta' = -I^{ns}_{1\pi+}(-\eta) + I_{1o}(\eta) + e^{j\eta s} I_{1+}(\eta) - e^{j\eta_o s} I^{ns}_{1+}(\eta) \tag{6.4}$$

with non-standard parts defined as in (6.2). The same contour integration on the right-hand side (RHS) of (6.3) yields

$$\frac{1}{2\pi j}\int_{\gamma_1} \frac{Y_c(\eta') V_{1o}(\eta')}{\eta' - \eta} d\eta' = Y_c(\eta) V_{1o}(\eta) + \frac{1}{2\pi j}\int_{-\infty}^{\infty} \frac{[Y_c(\eta') - Y_c(\eta)] V_{1o}(\eta')}{\eta' - \eta} d\eta'. \tag{6.5}$$

Notice that while performing contour integration we consider that no singularity is present along the path, due to the location of the physical poles (η_{go}) and the branch points $\eta = \pm k$, see §2.

Equation (6.5) is obtained by subtracting and summing $\frac{1}{2\pi j}\int_{\gamma_2} \frac{Y_c(\eta) V_{1o}(\eta')}{\eta' - \eta} d\eta'$ and considering (6.1) and (6.2) respectively in the two first integral terms and in the third one, which results in null ($V_{1o}(\eta)$ is thus entire without the non-standard part and for plus function the contours are closed in the upper half plane).

In (6.4), we have considered that the closure of the contour γ_1 for integrands $-I_{1\pi+}(-\eta)$, $I_{1o}(\eta)$, $e^{j\eta s} I_{1+}(\eta)$ (respectively minus, plus-entire and plus unknowns) is correspondingly performed in the lower, upper and upper half-planes (6.2), due to the convergence properties of the corresponding Laplace transform integrals (see §2) and considering the exponential factor $e^{j\eta s}$.

Equating (6.4) to (6.5), we get the regularized integral representation of (6.3):

$$I_{1o}(\eta) + e^{j\eta s} I_{1+}(\eta) - e^{j\eta_o s} I^{ns}_{1+}(\eta) - I^{ns}_{1\pi+}(-\eta) = Y_c(\eta) V_{1o}(\eta) + \frac{1}{2\pi j}\int_{-\infty}^{\infty} \frac{[Y_c(\eta') - Y_c(\eta)] V_{1o}(\eta')}{\eta' - \eta} d\eta' \tag{6.6}$$

that presents only plus and plus-entire unknowns together with non-standard source terms, while the minus unknown $I_{1\pi+}(-\eta)$ is eliminated.

Considering the second equation of (5.1)

$$-I_{1\pi+}(\eta) + I_{1o}(-\eta) + e^{-j\eta s} I_{1+}(-\eta) = Y_c(\eta) V_{1o}(-\eta) \tag{6.7}$$

we have a slightly different procedure. The application of the smile contour γ_1 integration (6.2) to the left hand side (LHS) of (6.7) yields

$$\frac{1}{2\pi j}\int_{\gamma_1} \frac{-I_{1\pi+}(\eta) + I_{1o}(-\eta) + e^{-j\eta s} I_{1+}(-\eta)}{\eta' - \eta} d\eta' = -I_{1\pi+}(\eta) + I^{ns}_{1\pi+}(\eta) + e^{j\eta_o s} I^{ns}_{1+}(-\eta) \tag{6.8}$$

where we have considered that for integrands $-I_{1\pi+}(\eta)$, $I_{1o}(-\eta)$, $e^{-j\eta s} I_{1+}(-\eta)$ (respectively plus, minus-entire and minus unknowns) the closure of the integration contour γ_1 is correspondingly

performed in the upper, lower and lower half-planes (6.2), due to the convergence properties of the corresponding Laplace transform integrals (see §2) and considering the exponential factor $e^{j\eta s}$. Note that in this case the contribution of $I_{1o}(-\eta)$ is null ($I_{1o}(-\eta)$ is a minus-entire function according to the definition of plus-entire functions given at the end of §2). On the right-hand side (RHS) of (6.7) the γ_1 contour integration yields

$$\frac{1}{2\pi j}\int_{\gamma_1}\frac{Y_c(\eta')V_{1o}(-\eta')}{\eta'-\eta}d\eta' = \frac{1}{2\pi j}\int_{-\infty}^{\infty}\frac{[Y_c(\eta')-Y_c(\eta)]V_{1o}(\eta')}{\eta'+\eta}d\eta' \tag{6.9}$$

by subtracting and summing $\frac{1}{2\pi j}\int_{\gamma_1}\frac{Y_c(\eta)V_{1o}(-\eta')}{\eta'-\eta}d\eta'$, using (6.1) and (6.2) respectively in the two first integral terms and in the third one (we performed closure of integration contours in the lower half planes for minus integrands and changed the sign of the integration variable).

Equating (6.8) to (6.9), we get the regularized integral representation of (6.7):

$$-I_{1\pi+}(\eta)+I^{ns}_{1\pi+}(\eta)+e^{j\eta_o s}I^{ns}_{1+}(-\eta)=\frac{1}{2\pi j}\int_{-\infty}^{\infty}\frac{[Y_c(\eta')-Y_c(\eta)]V_{1o}(\eta')}{\eta'+\eta}d\eta' \tag{6.10}$$

that presents only plus and plus-entire unknowns together with non-standard source terms, while the minus and minus-entire unknowns $I_{1\pi+}(-\eta)$, $I_{1o}(-\eta)$ are eliminated.

Without loss of completeness we can repeat the procedures highlighted for the first two equations of (5.1) to the other six getting similar integral representations. Equation (6.11) and (6.12) report two blocks of integral representations corresponding respectively to the first two blocks of the WH equation (5.1) and they present only plus and plus-entire unknowns after elimination of all minus and minus-entire unknowns.

$$\begin{cases} I_{1o}(\eta)+e^{j\eta s}I_{1+}(\eta)-e^{j\eta_o s}I^{ns}_{1+}(\eta)-I^{ns}_{1\pi+}(-\eta)=Y_c(\eta)V_{1o}(\eta)+\frac{1}{2\pi j}\int_{-\infty}^{\infty}\frac{[Y_c(\eta')-Y_c(\eta)]V_{1o}(\eta')}{\eta'-\eta}d\eta'. \\ -I_{1\pi+}(\eta)+I^{ns}_{1\pi+}(\eta)+e^{j\eta_o s}I^{ns}_{1+}(-\eta)=\frac{1}{2\pi j}\int_{-\infty}^{\infty}\frac{[Y_c(\eta')-Y_c(\eta)]V_{1o}(\eta')}{\eta'+\eta}d\eta'. \\ -e^{j\eta s}I_{1\pi+}(\eta)+e^{-j\eta_o s}I^{ns}_{1\pi+}(\eta)+I_{1\pi o}(\eta)+I^{ns}_{1+}(-\eta)=Y_c(\eta)V_{1\pi o}(\eta)+\frac{1}{2\pi j}\int_{-\infty}^{\infty}\frac{[Y_c(\eta')-Y_c(\eta)]V_{1\pi o}(\eta')}{\eta'-\eta}d\eta'. \\ -e^{-j\eta_o s}I^{ns}_{1\pi+}(-\eta)+I_{1+}(\eta)-I^{ns}_{1+}(\eta)=\frac{1}{2\pi j}\int_{-\infty}^{\infty}\frac{[Y_c(\eta)-Y_c(\eta')]V_{1\pi o}(\eta')]}{\eta'+\eta}d\eta'. \end{cases} \tag{6.11}$$

$$\begin{cases} -I_{2o}(\eta)-e^{j\eta s}I_{2+}(\eta)+e^{j\eta_o s}I^{ns}_{2+}(\eta)+I^{ns}_{2\pi+}(-\eta)=Y_c(\eta)V_{2o}(\eta)+\frac{1}{2\pi j}\int_{-\infty}^{\infty}\frac{[Y_c(\eta')-Y_c(\eta)]V_{2o}(\eta')}{\eta'-\eta}d\eta'. \\ -e^{j\eta_o s}I^{ns}_{2+}(-\eta)+I_{2\pi+}(\eta)-I^{ns}_{2\pi+}(\eta)=\frac{1}{2\pi j}\int_{-\infty}^{\infty}\frac{[Y_c(\eta)-Y_c(\eta')]V_{2o}(\eta')}{\eta'+\eta}d\eta'. \\ e^{j\eta s}I_{2\pi+}(\eta)-e^{-j\eta_o s}I^{ns}_{2\pi+}(\eta)-I_{2\pi o}(\eta)-I^{ns}_{2+}(-\eta)=Y_c(\eta)V_{2\pi o}(\eta)+\frac{1}{2\pi j}\int_{-\infty}^{\infty}\frac{[Y_c(\eta')-Y_c(\eta)]V_{2\pi o}(\eta')}{\eta'-\eta}d\eta'. \\ +e^{-j\eta_o s}I^{ns}_{2\pi+}(-\eta)-I_{2+}(\eta)+I^{ns}_{2+}(\eta)=\frac{1}{2\pi j}\int_{-\infty}^{\infty}\frac{[Y_c(\eta)-Y_c(\eta')]V_{2\pi o}(\eta')]}{\eta'+\eta}d\eta'. \end{cases} \tag{6.12}$$

(b) Application to complete WH equations: region 3

In region 3, explicit completed WH equations are derived by solving incompleteness in terms of a series of sampled spectral unknowns, see third block in (5.1) with (5.3), (5.2) and (4.8). As per the modified WH equations of regions 1 and 2, we exploit again the regularity properties of all reported entire WH unknowns in the set of non-redundant equations for the solution of

the problem. Since the third block in (5.1) contains only plus-entire unknowns, the procedure highlighted in the previous subsection is not required, i.e. the contour integration to eliminate all minus unknowns[1]. In order to avoid sampled spectral unknowns in the formulation, we apply a special version of the integral Cauchy representation formula. Equation (6.13) reports the special application of the integral Cauchy representation formula to a generic plus-entire function $F_o(\eta)$ estimated at $\eta = -\eta_n$:

$$F_o(-\eta_n) = \frac{1}{2\pi j}\int_{\gamma_1} \frac{F_o(\eta')}{\eta' + \eta_n} d\eta' = \frac{1}{2\pi j}\int_{-\infty}^{\infty} \frac{F_o(\eta')}{\eta' + \eta_n} d\eta', \quad n \in \mathbb{N}_0 \tag{6.13}$$

where γ_1 is the smile integration line and $\eta' = -\eta_n$ are the required samples located in the upper half-plane. Once the sampled plus entire spectral unknowns (5.3) have been represented in terms of (6.13), the third block in (5.1) becomes integral representations with a series of integral terms (according to n), i.e. (5.3) in (5.1) becomes:

$$\begin{aligned}
I_{s1_o}(\eta) &= \frac{1}{2\pi j}\int_{-\infty}^{\infty} [H_{11}(\eta,\eta')V_{1_o}(\eta') + H_{12}(\eta,\eta')V_{2_o}(\eta') \\
&\quad + H_{13}(\eta,\eta')V_{1\pi_o}(\eta') + H_{14}(\eta,\eta')V_{2\pi_o}(\eta')]d\eta' \\
I_{s2_o}(\eta) &= \frac{1}{2\pi j}\int_{-\infty}^{\infty} [H_{21}(\eta,\eta')V_{1_o}(\eta') + H_{22}(\eta,\eta')V_{2_o}(\eta') \\
&\quad + H_{23}(\eta,\eta')V_{1\pi_o}(\eta') + H_{24}(\eta,\eta')V_{2\pi_o}(\eta')]d\eta' \\
I_{s\pi 1_o}(\eta) &= \frac{1}{2\pi j}\int_{-\infty}^{\infty} [H_{31}(\eta,\eta')V_{1_o}(\eta') + H_{32}(\eta,\eta')V_{2_o}(\eta') \\
&\quad + H_{33}(\eta,\eta')V_{1\pi_o}(\eta') + H_{34}(\eta,\eta')V_{2\pi_o}(\eta')]d\eta' \\
I_{s2\pi_o}(\eta) &= \frac{1}{2\pi j}\int_{-\infty}^{\infty} [H_{41}(\eta,\eta')V_{1_o}(\eta') + H_{42}(\eta,\eta')V_{2_o}(\eta') \\
&\quad + H_{43}(\eta,\eta')V_{1\pi_o}(\eta') + H_{44}(\eta,\eta')V_{2\pi_o}(\eta')]d\eta'
\end{aligned} \tag{6.14}$$

with

$$H_{ij}(\eta,\eta') = \sum_{n=1}^{\infty} \frac{h_{ij}(\eta,n)}{t+\eta_n}, \; i,j = 1,2,3,4. \tag{6.15}$$

(c) Building the Fredholm integral equations of the problem

The key role in the method is performed by the application of the Cauchy representations to the spectral samples of the plus-entire unknowns, that is perfectly integrated into the Fredholm factorization method. In fact, after collecting the 12 integral representations reported in the three blocks constituted of (6.11), (6.12) and the third block in (5.1) with (6.14), we eliminate the current

[1]In case a problem presents a mixture of plus/plus-entire unknowns with minus/minus-entire unknowns together with sampled unknowns the procedure requires contour integration for the elimination of the minus unknowns as outlined in §6a.

unknowns $(I_{i+}(\eta), I_{i\pi+}(\eta), I_{io}(\eta), I_{i\pi o}(\eta); i = 1, 2)$ by substitution, yielding a system of Fredholm integral equations of the second kind of dimension four in terms of the voltage entire unknowns $(V_{io}(\eta), V_{i\pi o}(\eta); i = 1, 2)$.

$$
\begin{aligned}
&[Y_c(\eta) + Y_{11}(\eta)]V_{1o}(\eta) + Y_{12}(\eta)V_{2o}(\eta) + \frac{1}{2\pi j}\int_{-\infty}^{\infty}[(p(\eta,\eta') + H_{11}(\eta,\eta'))V_{1o}(\eta') + H_{12}(\eta,\eta')V_{2o}(\eta') \\
&\quad + (H_{13}(\eta,\eta') - e^{j\eta s}q(\eta,\eta'))V_{1\pi o}(\eta') + H_{14}(\eta,\eta')V_{2\pi o}(\eta')]d\eta' = n_1(\eta) \\
&Y_{21}(\eta)V_{1o}(\eta) + [Y_c(\eta) + Y_{22}(\eta)]V_{2o}(\eta) + \frac{1}{2\pi j}\int_{-\infty}^{\infty}[H_{21}(\eta,\eta')V_{1o}(\eta') + (p(\eta,\eta') + H_{22}(\eta,\eta'))V_{2o}(\eta') \\
&\quad + H_{23}(\eta,\eta')V_{1\pi o}(\eta') + (H_{24}(\eta,\eta') - e^{j\eta s}q(\eta,\eta'))V_{2\pi o}(\eta')]d\eta' = n_2(\eta) \\
&[Y_c(\eta) + Y_{11}(\eta)]V_{1\pi o}(\eta) + Y_{12}(\eta)V_{2\pi o}(\eta) + \frac{1}{2\pi j}\int_{-\infty}^{\infty}[(H_{31}(\eta,\eta') - e^{j\eta s}q(\eta,\eta'))V_{1o}(\eta') \\
&\quad + H_{32}(\eta,\eta')V_{2o}(\eta') + (p(\eta,\eta') + H_{33}(\eta,\eta'))V_{1\pi o}(\eta') + H_{44}(\eta,\eta')V_{2\pi o}(\eta')]d\eta' = n_3(\eta) \\
&Y_{21}(\eta)V_{1\pi o}(\eta) + [Y_c(\eta) + Y_{22}(\eta)]V_{2\pi o}(\eta) + \frac{1}{2\pi j}\int_{-\infty}^{\infty}[H_{41}(\eta,\eta')V_{1o}(\eta') \\
&\quad + (H_{42}(\eta,\eta') - e^{j\eta s}q(\eta,\eta'))V_{2o}(\eta') + H_{43}(\eta,\eta')V_{1\pi o}(\eta') + (p(\eta,\eta') \\
&\quad + H_{44}(\eta,\eta'))V_{2\pi o}(\eta')]d\eta' = n_4(\eta)
\end{aligned}
\tag{6.16}
$$

with

$$
p(\eta,\eta') = \frac{Y_c(\eta') - Y_c(\eta)}{\eta' - \eta}, \quad q(\eta,\eta') = -\frac{Y_c(\eta') - Y_c(\eta)}{\eta' + \eta} \tag{6.17}
$$

and

$$
\begin{aligned}
n_1(\eta) &= (e^{j\eta s} - e^{j\eta_o s})I^{ns}_{1+}(\eta) + (e^{j(\eta-\eta_o)s} - 1)I^{ns}_{1\pi+}(-\eta), \\
n_2(\eta) &= (e^{j\eta_o s} - e^{j\eta s})I^{ns}_{2+}(\eta) + (1 - e^{j(\eta-\eta_o)s})I^{ns}_{2\pi+}(-\eta), \\
n_3(\eta) &= (1 - e^{j(\eta+\eta_o)s})I^{ns}_{1+}(-\eta) + (e^{-j\eta_o s} - e^{j\eta s})I^{ns}_{1\pi+}(\eta), \\
n_4(\eta) &= (e^{j(\eta+\eta_o)s} - 1)I^{ns}_{2+}(-\eta) + (e^{j\eta s} - e^{-j\eta_o s})I^{ns}_{2\pi+}(\eta).
\end{aligned}
\tag{6.18}
$$

The series of integral terms derived by the Cauchy representations (6.14) with (6.15) augment the compact kernels present in (6.11), (6.12), preserving convergence properties, thus the formulation is regularized. We get (6.16)–(6.18). Equations (6.16) are non-homogeneous equations unlike the original WH equation (5.1), as the application of the fundamental Cauchy decomposition formula (6.2) to (5.1) has extracted the source $n_i(\eta)$ (η) (6.18). These terms are non-standard contributions of the WH unknowns defined in terms of GO field components.

The final set of Fredholm integral equations can be written in compact form as follows:

$$
\underline{V}_o(\eta) = \frac{1}{2\pi j}\int_{-\infty}^{\infty}\underline{\underline{K}}(\eta,\eta')\underline{V}_o(\eta')d\eta' + \underline{s}(\eta) \tag{6.19}
$$

with $\eta \in \mathbb{R}$ and where the vector $\underline{V}_o(\eta) = [V_{1o}(\eta), V_{2o}(\eta), V_{1\pi o}(\eta), V_{2\pi o}(\eta)]^t$, the matrix $\underline{\underline{K}}(\eta,\eta')$ contains the kernels and the vector $\underline{s}(\eta)$ is the known term on the right hand side due to sources (non-standard terms). In case of plane wave illumination from region 1 we have to consider in

$\underline{s}(\eta)$ and $(n_i(\eta))$ (6.18) only non-standard terms of $I_{1+}(\eta), I_{1\pi+}(\eta)$ due to the incident wave and the reflected wave:

$$H_x^g(\rho,\varphi) = -\frac{E_o}{Z_o}\sin(\varphi_o)e^{jk\rho\cos(\varphi-\varphi_o)} + \frac{E_o}{Z_o}\sin(\varphi_o)e^{jk\rho\cos(\varphi+\varphi_o)}. \tag{6.20}$$

According to (2.3)–(2.5) (see also (2.13)) it yields:

$$I_{1+}^{ns}(\eta) = -\frac{2jE_o\sin(\varphi_o)e^{-j\eta_o s}}{Z_o(\eta-\eta_o)}, \quad I_{1\pi+}^{ns}(\eta) = \frac{2jE_o\sin(\varphi_o)}{Z_o(\eta+\eta_o)}. \tag{6.21}$$

Note that the kernel $\underline{\underline{K}}(\eta,\eta')$ contains a series of terms depending on $H_{ij}(\eta,\eta')$, see (6.15), that requires truncation at some N during implementation. Such truncation can be guided by the number of propagating/non-propagating modes we want to consider to represent the field in region 3, according to η_n (4.1).

Equation (6.16) and (6.19) are complete and explicit systems of Fredholm integral equations of the second kind, in particular, we resort to the theory reported in the Appendix of [68] inspired by [69] to demonstrate that (6.19) is with compact kernel considering a suitable generalized Hilbert space. Thus, simple numerical quadratures, such as sample-and-hold, allow us to obtain an approximate version of (6.19) from which we get approximate solutions [46] with the reconstruction formula. We recall that the integration is performed along the real axis to avoid any divergence in exponential terms and to avoid crossing any of the source/structural singularities, which are located in the 2nd and 4th quadrants.

7. Numerical results and validation

To validate the proposed technique we examine in detail the representative electromagnetic scattering problem of a slot in a thick metallic screen illuminated by plane-waves (figure 1), whose formulation is reported in detail in the previous sections.

In the following, we present self-convergence tests and validation through an independent fully numerical solution based on finite methods embedding singular modelling [59–62] with the help of the open source specialized library for singular quadrature reported in [70,71].

We consider the reference problem of figure 1 illuminated by an E_z plane wave (2.3) with the following parameters: $E_o = 1V/m$, $k = k_r - jk_r/10000$, $\varphi_o = 2\pi/9$ rad, $k_r d = 2$, $k_r s = 7$, and we assume a normalized value $k_r = 1$ for graphics about spectra.

We examine self-convergence in terms of spectral solutions of the relevant Fredholm equation (6.19) and we validate the solution against the finite element method by computing GTD field components and total far field via asymptotics applied on the semi-analytical spectral solution proposed in this work.

In the following, we consider as a reference solution the one obtained with sample-and-hold quadrature in (6.19) with truncation of the integration interval $A = 40$ (i.e. the integration interval is $\eta \in [-A, A]$), integration step $h = 0.05$, number of η_n to be considered in the augmented kernel $N = 15$ (as discussed in §6b,c with (6.15)) for a convergent solution.

At the top of figure 2, we show the spectrum $V_{1o}(\eta), e^{j\eta s}V_{1\pi o}(-\eta), V_{2o}(\eta), e^{j\eta s}V_{2\pi o}(-\eta)$ (according to (2.10)) for real η obtained for the reference solution. In the central part of figure 2, we show the relative errors in $\log_{10}$ scale among the representations with π auxiliary functions and with the original entire functions. The central subfigures demonstrate the coincidence of representations and the symmetry of the formulation reaching relative errors of approximately machine level, and it constitutes a first validation of the correctness of the equations. At the bottom of figure 2, we have the self-convergence validation analysing the relative errors in log 10 scale for $V_{1o}(\eta), V_{2o}(\eta)$ with various A, h and fixed $N = 10$ with respect to the reference solution ($A = 40$, $h = 0.05$, $N = 15$). The bottom subfigures shows self-convergence, in particular in the spectral zone where the relevant spectrum is significant.

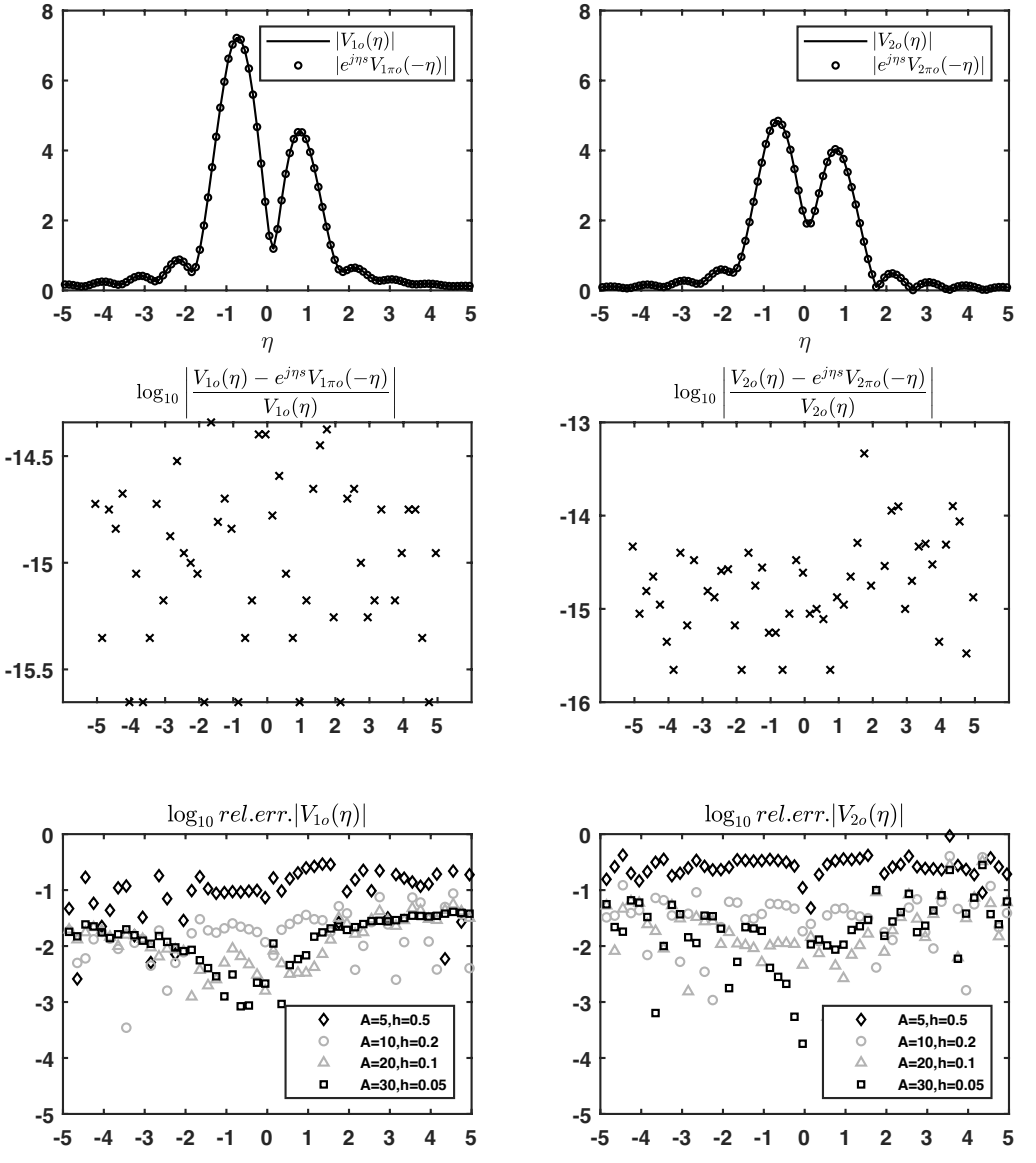

Figure 2. Thick slot illuminated by an E_z plane wave with $E_o = 1V/m$, $k = k_r - jk_r/10000$, $\varphi_o = 2\pi/9$ rad, $k_r d = 2$, $k_r s = 7$ (we assume a normalized value $k_r = 1$). The top left (right) subfigure reports the absolute value of $V_{1o}(\eta)$ and $e^{j\eta s}V_{1\pi o}(-\eta)$ ($V_{2o}(\eta)$ and $e^{j\eta s}V_{2\pi o}(-\eta)$ for the reference solution obtained with $A = 40$, $h = 0.05$, $N = 15$. The central left (right) subfigure reports the respective relative error in $\log_{10}$ among the two evaluations: the coincidence of the two representations from relative errors reaching almost machine precision is clear. The bottom left (right) subfigure reports the relative errors in $\log_{10}$ on the computation of $V_{1o}(\eta)$ ($V_{2o}(\eta)$) with various A, h and fixed $N = 10$ with respect to the reference solution.

Figure 3 shows the spectrum $V_{1o}(\eta), V_{2o}(\eta)$ for real η obtained for the reference solution ($A = 40$, $h = 0.05$, $N = 15$) and for solutions with fixed $A = 20, h = 0.1$ and various $N = 0, 1, 2, 10$. The bottom of figure 3 shows the relative errors in $\log_{10}$ on the computation of $V_{1o}(\eta), V_{2o}(\eta)$ with fixed $A = 20, h = 0.1$ and $N = 0, 1, 2, 10$ with respect to the reference solution. Figure 3 demonstrates convergence in particular for the chosen number of N.

The proposed simulations (figures 2 and 3) demonstrate self-convergence according to all three different parameters of computation A, h, N.

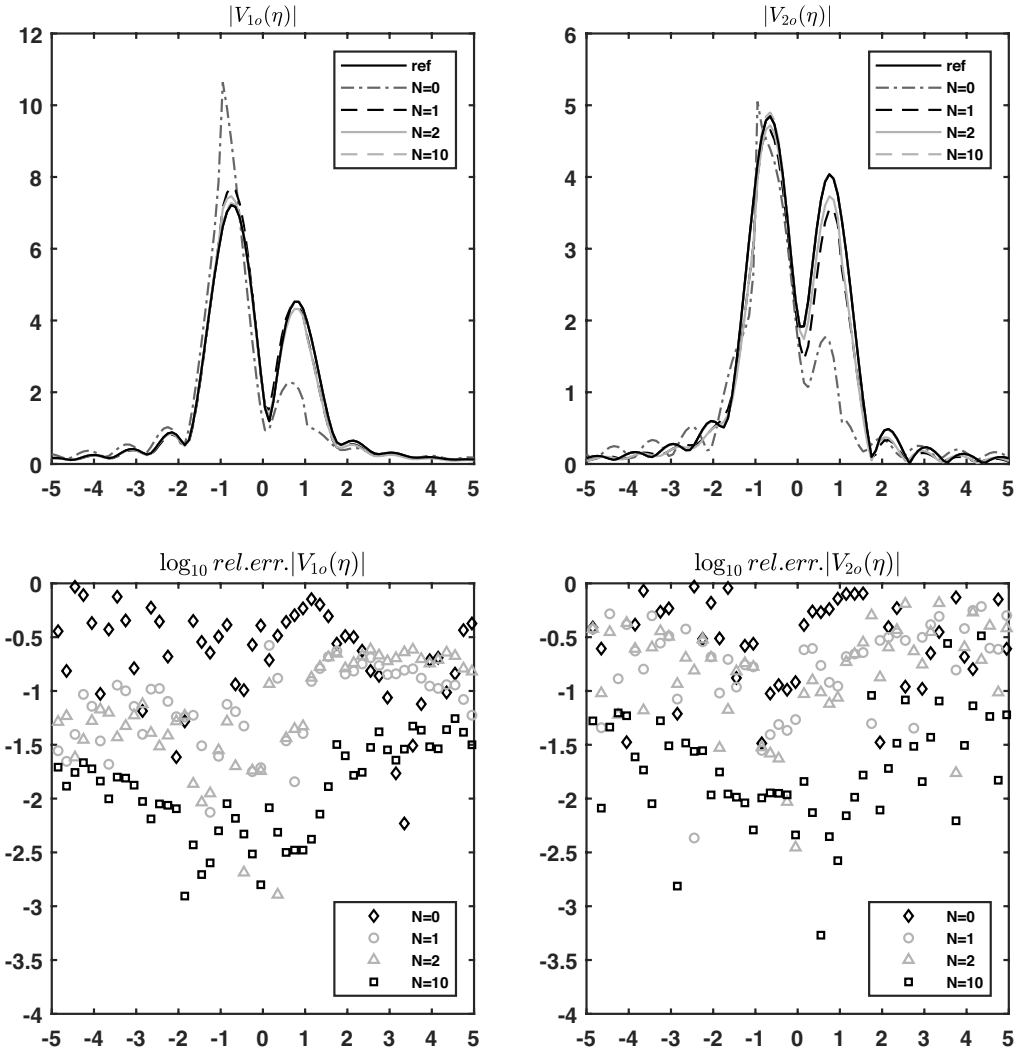

Figure 3. Thick slot illuminated by an E_z plane wave with $E_o = 1V/m$, $k = k_r - jk_r/10000$, $\varphi_o = 2\pi/9$ rad, $k_r d = 2$, $k_r s = 7$ (we assume a normalized value $k_r = 1$). The top left (right) subfigure reports the absolute value of $V_{1o}(\eta)$ ($V_{2o}(\eta)$) for the reference solution obtained with $A = 40$, $h = 0.05$, $N = 15$ and for solutions with $A = 20$, $h = 0.1$ and $N = 0, 1, 2, 10$. The bottom left (right) subfigure reports the relative errors in $\log_{10}$ on the computation of $V_{1o}(\eta)$ ($V_{2o}(\eta)$) with fixed $A = 20$, $h = 0.1$ and various N with respect to the reference solution.

To further validate the method we compare our reference solution with the one obtained with finite element methods embedding singular modelling [59] and implementing the singular quadrature [71] with the following setup: regions 1 and 2 are truncated at a distance of 30λ respectively from the origin A' and A'' (figure 1) with a semi-cylindrical shaped perfectly matched layer (PML) of depth $\lambda/2$, and the geometrical domain is discretized with curvilinear 2nd order triangular elements of maximum side length $\lambda/10$.

We compare the GTD field and total far field obtained at $k\rho = 10$ with respect to A' and A'' (figure 1) respectively in regions 1 and 2. For what concerns the evaluation of GTD field components from spectral solutions, we apply the saddle point technique to the spectra derived for the two reference systems related to the two regions. From $V_{1o}(\eta)$, $V_{2o}(\eta)$, we compute the spectra for

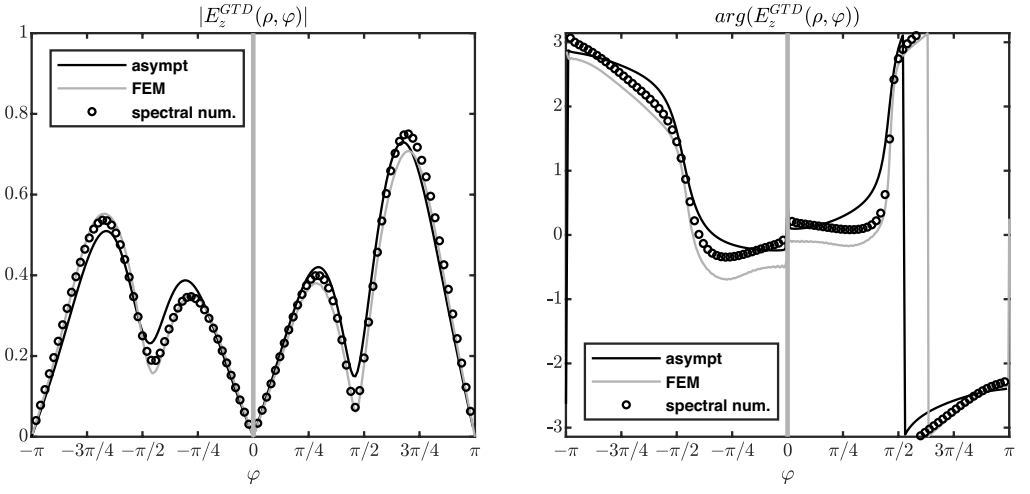

Figure 4. Thick slot illuminated by an E_z plane wave with $E_o = 1V/m$, $k = k_r - jk_r/10000$, $\varphi_o = 2\pi/9$ rad, $k_r d = 2$, $k_r s = 7$ (we assume a normalized value $k_r = 1$). GTD field for the test problem under consideration respectively for region 1 at $k\rho = 10$ from A' and for region 2 at $k\rho = 10$ from A''. Left (right): Comparison among absolute value (phase) of GTD field estimated via asymptotics (7.3), (7.5) from the obtained reference spectral solution ($A = 40$, $h = 0.05$, $N = 15$), via finite element simulation and via the application of adaptive numerical integration in the inverse transforms (7.2) of the reference spectral solution along the real axis η.

the reference systems respectively centred at A' and A'' (figure 1), and obtain:

$$V_{1o}^{A'}(\eta) = e^{-j\eta s/2} V_{1o}(\eta)$$
$$V_{2o}^{A''}(\eta) = e^{-j\eta s/2} V_{2o}(\eta) \tag{7.1}$$

This redefinition of spectra is of major importance for the correct computation of phase in fields.

The diffracted contribution derives from the inverse Laplace formula applied to the entire voltage spectra $V_{1o}^{A'}(\eta)$, $V_{2o}^{A''}(\eta)$ that we estimate warping the integration contour (real axis) into the SDP path

$$E_z^d(x,y) = \frac{1}{2\pi_-}\int_{-\infty}^{\infty} V_{1o}^{A'}(\eta) e^{-j\xi(\eta)y} e^{-j\eta(x-\frac{s}{2})} d\eta = -\frac{1}{2\pi_-}\int_{SDP} V_{1o}^{A'}(\eta) e^{-j\xi(\eta)y} e^{-j\eta(x-\frac{s}{2})} d\eta,\ y > 0$$
$$E_z^d(x,y) = \frac{1}{2\pi_-}\int_{-\infty}^{\infty} V_{2o}^{A''}(\eta) e^{+j\xi(\eta)(y+d)} e^{-j\eta(x-\frac{s}{2})} d\eta = -\frac{1}{2\pi_-}\int_{SDP} V_{2o}^{A''}(\eta) e^{+j\xi(\eta)(y+d)} e^{-j\eta(x-\frac{s}{2})} d\eta,\ y < -d. \tag{7.2}$$

At far field in region 1, we approximate the first integral of (7.2) only with the evaluation of the integrand at the saddle point ($\eta_s = k\cos\varphi$), that provides the GTD field component

$$E_z^{GTD}(\rho,\varphi) = \sqrt{\frac{k}{2\pi\rho}} e^{-j(k\rho-\pi/4)} V_{1o}^{A'}(k\cos\varphi)\sin\varphi, \quad 0 < \varphi < \pi \tag{7.3}$$

where the cylindrical coordinates are defined with respect to the origin A' (figure 1). For what concerns the GO field in region 1 we have

$$E_z^g(\rho,\varphi) = E_o e^{-jk\rho\cos(\varphi-\varphi_o)} - E_o e^{-jk\rho\cos(\varphi+\varphi_o)}, \quad 0 < \varphi < \pi \tag{7.4}$$

with respect to the phase centre A'.

Similarly in region 2, we have the GTD field component

$$E_z^{GTD}(\rho,\varphi) = \sqrt{\frac{k}{2\pi\rho}} e^{-j(k\rho-\pi/4)} V_{2o}^{A''}(k\cos\varphi)|\sin\varphi|, \quad -\pi < \varphi < 0 \tag{7.5}$$

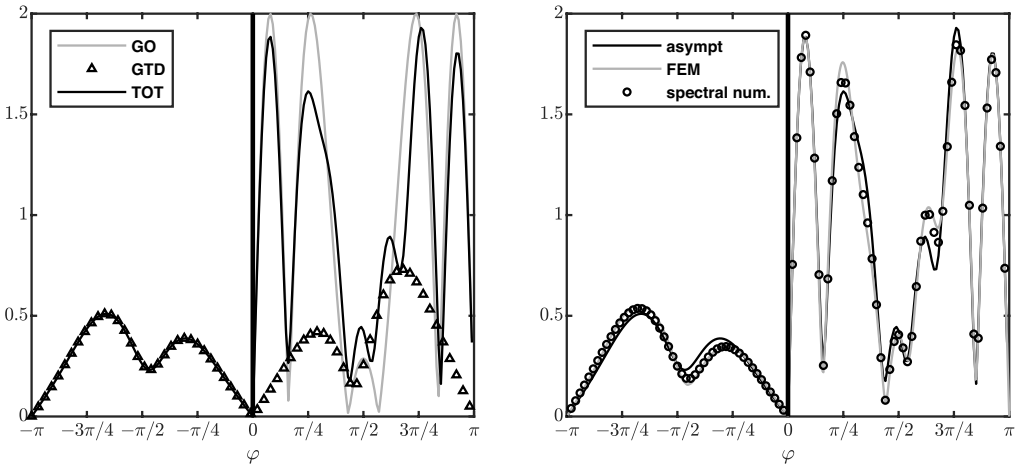

Figure 5. Thick slot illuminated by an E_z plane wave with $E_o = 1V/m, k = k_r - jk_r/10000, \varphi_o = 2\pi/9$ rad, $k_r d = 2, k_r s = 7$ (we assume a normalized value $k_r = 1$). Left: GO component (7.4), GTD component (7.3), (7.5) and total far field at $k_r\rho = 10$ obtained by asymptotic estimations applied to the reference spectral semi-analytical solution ($A = 40, h = 0.05, N = 15$). Right: the total far field of our solution is compared with the one obtained with the finite element method and the one obtained using numerical integration of the inverse Laplace transformation of our semi-analytical spectral reference solution.

where the cylindrical coordinates are defined with respect to the origin A'' (figure 1) and the GO component is null as we illuminate region 1 only.

Figure 4 reports the GTD component of the field for the validation problem, by considering for regions 1 and 2 respectively a distance from the origins A' and A'' of $k\rho = 10$. The figure reports, in terms of absolute value and phase, the comparison among (i) the asymptotic GTD field (7.3), (7.5) estimated from the obtained reference spectral solution ($A = 40, h = 0.05, N = 15$), (ii) the GTD field obtained from finite element simulation and (iii) the one obtained by applying adaptive numerical integration in the inverse transforms (7.2) of the reference spectral solution along the real axis η. We notice the coincidence among the three presented results in terms of absolute value and phase. We recall that the phase is a very sensitive parameter to check the quality of convergence in comparison to the absolute value.

We also report an incomparable advantage in terms of computational time for our semi-analytical-spectral solution combined with asymptotic analysis with respect to full numerical techniques and hybrid computations as performed in the numerical integration for the inverse Laplace transformation of the semi-analytical spectral solutions.

Figure 5 reports on the left our reference solution ($A = 40, h = 0.05, N = 15$) after asymptotic evaluation in terms of field components at $k_r\rho = 10$: GO component (7.4), GTD component (7.3), (7.5) and total far field which is the sum of the two previous components. On the right side of the same figure, the total far field of our solution is compared with the one obtained with the finite element method and the one obtained using numerical integration in the inverse Laplace transformation of our semi-analytical spectral reference solution. Again the lines of the figure almost overlap, providing a validation of the obtained results.

8. Conclusion

This paper presents an innovative, versatile, general, completed, not-specialized effective semi-analytical method to deal with problems formulated in terms of Wiener–Hopf equations which contain entire unknowns and exponential phase factors. The methodology reduces the factorization problem to regularized integral equations and does not require either any pre-factorization of kernels and/or solutions of systems of infinite equations with no physical interpretation. The

key role in the method is represented by a particular application of the Fredholm factorization method combined with the Cauchy integral representation formula that allows us to remedy the incompleteness of the Wiener–Hopf formulation providing a complete exact Wiener–Hopf modelling. The method systematically yields Fredholm integral equations of the second kind with augmented kernel that are explicit in terms of the spectral physical unknowns of the problem, therefore it provides regularized integral equation formulations. The solution of integral equations is semi-analytical in spectral domain with simple quadrature formula that allows asymptotic estimation of field components similarly to what is done in problems with available closed-form spectral solutions.

In particular, we validate the method analysing a practical application in electromagnetism: the scattering of a plane wave by a slot in a thick metallic screen. The simplicity of the proposed reference validation test case does not limit the applicability of the method in more complex problems where impenetrable/penetrable boundary conditions, finite dimension regions and localized sources are considered, but the technical details of the application to these problems go beyond the scope of this fundamental methodological paper.

The paper also provides an innovative method to obtain systematically the Wiener–Hopf equations in spectral domain by partitioning the geometry of the problem and applying a systematic network interpretation of the formulation. In the paper, we demonstrate that the combination of these mathematical tools allows us to study the test problem in spectral domain with physical and engineering insights. Numerical results validate the proposed methodology.

Data accessibility. This article has no additional data.

Declaration of AI use. We have not used AI-assisted technologies in creating this article.

Authors' contributions. V.D.: conceptualization, data curation, formal analysis, investigation, methodology, software, validation, visualization, writing—original draft, writing—review and editing; G.L.: conceptualization, data curation, formal analysis, funding acquisition, investigation, methodology, project administration, software, validation, visualization, writing—original draft, writing—review and editing.

Both authors gave final approval for publication and agreed to be held accountable for the work performed therein.

Conflict of interest declaration. We declare we have no competing interests.

Funding. This work was supported by EU–Next Generation EU within PNRR M4C2, Investimento 1.4-Avviso n.3138 16/12/2021-CN00000013 National Centre for HPC, Big Data and Quantum Computing (HPC)-CUP E13C22000990001-Multiscale modeling and Engineering App.

References

1. Noble B. 1958 *Methods based on the Wiener-Hopf technique for the solution of partial differential equations*. London, UK: Pergamon Press.
2. Mittra R, Lee SW. 1971 *Analytical techniques in the theory of guided waves*. New York, NY, USA: MacMillan.
3. Kobayashi K. 2013 Solutions of wave scattering problems for a class of the modified Wiener-Hopf geometries. *IEEJ Trans. Fundam. Mater*. **133**, 233–241. (doi:10.1541/ieejfms.133.233)
4. Daniele V, Zich RS. 2014 *The Wiener-Hopf method in electromagnetics*. Raleigh, NC, USA: SciTech Publishing.
5. Daniele V, Lombardi G. 2016 Arbitrarily oriented perfectly conducting wedge over a dielectric half-space: diffraction and total far field. *IEEE Trans. Antennas Propag*. **371**, 1416–1433. (doi:10.1109/tap.2016.2524412)
6. Daniele VG, Lombardi G, Zich RS. 2017 The electromagnetic field for a PEC wedge over a grounded dielectric slab: 2. diffraction, modal field, surface waves, and leaky waves. *Radio Sci*. **52**, 1492–1509. (doi:10.1002/2017rs006388)
7. Daniele VG, Lombardi G, Zich RS. 2018 The scattering of electromagnetic waves by two opposite staggered perfectly electrically conducting half-planes. *Wave Motion* **83**, 241–263. (doi:10.1016/j.wavemoti.2018.09.017)

8. Daniele V, Lombardi G, Zich RS. 2019 Radiation and scattering of an arbitrarily flanged dielectric-loaded waveguide. *IEEE Trans. Antennas Propag.* **67**, 7569–7584. (doi:10.1109/tap.2019.2948494)
9. Daniele V, Lombardi G, Zich RS. 2022 Physical and spectral analysis of a semi-infinite grounded slab illuminated by plane waves. *IEEE Trans. Antennas Propag.* **70**, 12104–12119. (doi:10.1109/tap.2022.3210704)
10. Daniele V, Lombardi G. 2023 Completeness and regularization techniques for Wiener-Hopf problems with discontinuous layers. In *Proc. of 2023 17th European Conf. on Antennas and Propagation (EuCAP)*, Florence, Italy, pp. 1–4. Institute of Electrical and Electronics Engineers (IEEE). (doi:10.23919/EuCAP57121.2023.10133326)
11. Daniele VG, Lombardi G. 2021 The generalized Wiener–Hopf equations for wave motion in angular regions: electromagnetic application. *Proc. R. Soc. A* **477**, 1–27. (doi:10.1098/rspa.2021.0040)
12. Daniele V, Lombardi G. 2024 Spectral analysis of electromagnetic diffraction phenomena in angular regions filled by arbitrary linear media. *Appl. Sci.* **14**, 1–37. (doi:10.3390/app14198685)
13. Jones DS. 1952 Diffraction by a wave-guide of finite length. *Proc. Camb. Phil. Soc.* **48**, 118–134. (doi:10.1017/S0305004100027432)
14. Abrahams ID, Wickham GR. 1988 On the scattering of sound by two semi-infinite parallel staggered plates - I. explicit matrix Wiener-Hopf factorization. *Proc. R. Soc. Lond. A* **420**, 131–156. (doi:10.1098/rspa.1988.0121)
15. Jones DS. 1953 Diffraction by a thick semi-infinite plane. *Proc. R. Soc. Lond. A* **217**, 153–175.
16. Williams WE. 1954 Diffraction by two parallel planes of finite length. *Math. Proc. Camb. Phil. Soc.* **50**, 309–318. (doi:10.1017/s0305004100029388)
17. Jones DS. 1964 *The theory of electromagnetism*. New York, NY, USA: Pergamon.
18. Mittra R, Lee SW. 1970 On the solution of a generalized Wiener-Hopf equation. *J. Math. Phys.* **11**, 775–783. (doi:10.1063/1.1665209)
19. Kashyap S, Hamid M. 1971 Diffraction characteristics of a slit in a thick conducting screen. *IEEE Trans. Antennas Propag.* **19**, 499–507. (doi:10.1109/tap.1971.1139961)
20. Kashyap SC. 1974 Diffraction characteristics of a slit formed by two staggered parallel planes. *J. Math. Phys.* **15**, 1944–1949. (doi:10.1063/1.1666562)
21. Yoshidomi K, Aoki K, Uchida K. 1983 Diffraction of an electromagnetic plane wave by a slit in a lossy dielectric slab. *Electron. Commun. Jpn.* **66**, 81–90. (doi:10.1002/ecja.4400660811)
22. Kobayashi K. 1985 Diffraction of a plane electromagnetic wave by a parallel plate grating with dielectric loading: the case of transverse magnetic incidence. *Can. J. Phys.* **63**, 453–465. (doi:10.1139/p85-071)
23. Janaswamy R. 1990 Wiener-Hopf analysis of the asymmetric slotline. *Radio Sci.* **25**, 699–706. (doi:10.1029/rs025i005p00699)
24. Kobayashi K, Sawai A. 1992 Plane wave diffraction by an open-ended parallel plate waveguide cavity. *J. Electromagn. Waves Appl.* **6**, 475–512. (doi:10.1163/156939392x01264)
25. Hashimoto M, Idemen M, Tretyakov OA. 1993 Chapter 4-Some diffraction problems involving modified Wiener-Hopf geometries. In *Analytical and numerical methods in electromagnetic wave theory* (ed. K Kobayashi), pp. 147–228. Tokyo, Japan: Science House Co.
26. Koshikawa S, Kobayashi K. 1994 Wiener-Hopf analysis of the diffraction by a parallel-plate waveguide cavity with partial material loading. *IEICE Trans. Electron.* **77**, 975–985.
27. Birbir F, Büyükaksoy A. 1996 Plane wave diffraction by a wide slit in a thick impedance screen. *J. Electromagn. Waves Appl.* **10**, 803–826. (doi:10.1163/156939396x00793)
28. Polat B, Buyukaksoy A, Cinar G. 2001 Plane wave diffraction by tandem impedance slits. *PIER* **34**, 29–61. (doi:10.2528/PIER01022605)
29. Şahinkaya DSA, Büyükaksoy A. 2005 Diffraction by a rectangular groove with resistive walls. *AEU Int. J. Electron. Commun.* **59**, 55–58. (doi:10.1016/j.aeue.2004.11.001)
30. Tayyar IH, Büyükaksoy A, Işıkyer A. 2008 A Wiener-Hopf analysis of the parallel plate waveguide with finite length impedance loading. *Radio Sci.* **43**, 1–12. (doi:10.1029/2007rs003768)
31. Zheng JP, Kobayashi K. 2008 Plane wave diffraction by a finite parallel-plate waveguide with four-layer material loading: part I - the case of e polarization. *Prog. Electromagn. Res. B* **6**, 1–36. (doi:10.2528/pierb08031219)
32. Tayyar IH, Çolak B. 2017 Plane wave scattering by a dielectric loaded slit in a thick impedance screen. *J. Electromagn. Waves Appl.* **31**, 604–626. (doi:10.1080/09205071.2017.1300545)

33. Kobayashi K, Smith PD. 2020 Chapter 11-Wiener-Hopf analysis of the diffraction by a thin material strip | Takashi Nagasaka and Kazuya Kobayashi. In *Advances in mathematical methods for electromagnetics* (eds T Nagasaka, K Kobayashi), pp. 255–277. Stevenage, UK: SciTech Publishing. (doi:10.1049/SBEW528E_ch11)
34. Abrahams ID, Wickham GR. 1990 General Wiener–Hopf factorization of matrix kernels with exponential phase factors. *SIAM J. Appl. Math.* **50**, 819–838. (doi:10.1137/0150047)
35. Abrahams ID, Wickham GR. 1990 Acoustic scattering by two parallel slightly staggered rigid plates. *Wave Motion* **12**, 281–297. (doi:10.1016/0165-2125(90)90044-5)
36. Kisil AV. 2018 An Iterative Wiener–Hopf method for triangular matrix functions with exponential factors. *SIAM J. Appl. Math.* **78**, 45–62. (doi:10.1137/17m1136304)
37. Livasov P, Mishuris G. 2019 Numerical factorization of a matrix-function with exponential factors in an anti-plane problem for a crack with process zone. *Phil. Trans.R. Soc. A* **377**, 20190109. (doi:10.1098/rsta.2019.0109)
38. Priddin MJ, Kisil AV, Ayton LJ. 2019 Applying an iterative method numerically to solve n x n matrix Wiener–Hopf equations with exponential factors. *Phil. Trans. R. Soc. A* **378**. (doi:10.1098/rsta.2019.0241)
39. Friedman B. 1956 *Principles and techniques of applied mathematics*. New York, NY, USA: Wiley.
40. Mittag-Leffler G. 1884 Sur la représentation analytique des fonctions monogènes uniformes d'une variable indépendante. *Acta Math.* **4**, 1–79. (doi:10.1007/BF02418410)
41. Spiegel MR. 2009 *Complex variables with an introduction to conformal mapping and its applications*, 2nd edn. New York, NY, USA: McGraw Hill.
42. Daniele V, Lombardi G. 2007 Fredholm factorization of Wiener-Hopf scalar and matrix kernels. *Radio Sci.* **42**, 1–9. (doi:10.1029/2007rs003673)
43. Daniele V, Lombardi G. 2020 *Scattering and diffraction by wedges 1: the wiener-hopf solution—theory*. Hoboken, NJ, USA: Wiley. (doi:10.1002/9781119476733)
44. Daniele V, Lombardi G. 2006 Wiener-Hopf solution for impenetrable wedges at skew incidence. *IEEE Trans. Antennas Propag.* **54**, 2472–2485. (doi:10.1109/TAP.2006.880723)
45. Vekua NP. 1967 *System of singular integral equations*. Gronigen, The Netherlands: P. Noordhoff.
46. Kantorovich LV, Krylov VI. 1964 *Approximate methods of higher analysis*. Groningen, The Netherlands: Noordhoff.
47. Henke H, Fruchting H. 1976 Radiation in a slotted half space and diffraction by a slit in a thick screen. *Nachrichtentech. Z* **29**, 401.
48. Litvinenko LN, Prosvirnin SL, Shestopalov VP. 1977 Diffraction of a planar, H-polarized electromagnetic wave on a slit in a metallic shield of finite thickness. *Radio Eng. Electron. Phys.* **22**, 474–484.
49. Mata Mendez O, Cadilhac M, Petit R. 1983 Diffraction of a two-dimensional electromagnetic beam wave by a thick slit pierced in a perfectly conducting screen. *J. Opt. Soc. Am.* **73**, 328–331. (doi:10.1364/josa.73.000328)
50. Kang SH, Eom HJ, Park TJ. 1993 TM scattering from a slit in a thick conducting screen: revisited. *IEEE Trans. Microw. Theory Tech.* **41**, 895–899. (doi:10.1109/22.234533)
51. Eom HJ. 2001 *Wave scattering theory: a series approach based on the Fourier transformation*. Berlin, Germany: Springer-Verlag.
52. Haddab AH, Kuester EF. 2018 Extraordinary transmission through a single dielectric-loaded slot in a thick metallic shield. *IEEE Trans. Antennas Propag.* **66**, 1846–1853. (doi:10.1109/tap.2018.2800687)
53. Haddab AH, Kuester EF. 2020 The effect of inhomogeneous dielectric loading on transmission through a slot in an infinite thick metallic shield. *J. Electromagn. Waves Appl.* **34**, 759–773. (doi:10.1080/09205071.2020.1751733)
54. Hongo K, Ishii G. 1978 Diffraction of an electromagnetic plane wave by a thick slit. *IEEE Trans. Antennas Propag.* **26**, 494–499. (doi:10.1109/tap.1978.1141870)
55. Sato R, Shirai H. 1996 Plane wave diffraction by a thick slit-TE case. In *Proc. ISAP*, Chiba, Japan, vol. **96**, pp. 109–112, Seoul, South Korea: Institute of Electronics and Information Engineers.
56. Shirai H, Shimizu M, Sato R. 2016 Hybrid ray-mode analysis of e-polarized plane wave diffraction by a thick slit. *IEEE Trans. Antennas Propag.* **64**, 4828–4835. (doi:10.1109/tap.2016.2608978)
57. Nguyen KN, Shirai H. 2019 High frequency diffraction by thick loaded conducting slits–H polarization case. In *2019 IEEE Int. Symposium on Antennas and Propagation and USNC-URSI*

Radio Science Meeting, Atlanta, GA, USA, pp. 497–498. New York, NY: IEEE. (doi:10.1109/APUSNCURSINRSM.2019.8888920)
58. Nguyen KN, Shirai H, Serizawa H. 2021 Electromagnetic scattering analysis from a rectangular hole in a thick conducting screen. *IEICE Trans. Electron*. **104**, 134–143. (doi:10.1587/transele.2020rep0001)
59. Graglia RD, Lombardi G. 2004 Singular higher order complete vector bases for finite methods. *IEEE Trans. Antennas Propag.* **52**, 1672–1685. (doi:10.1109/TAP.2004.831292)
60. Graglia RD, Lombardi G, Wilton DR, Johnson WA. 2005 Modeling edge singularities in the method of moments. In *2005 IEEE Antennas and Propagation Society Int. Symposium*, Washington, DC, USA, vol. 3A, pp. 56–59, New York, NY: IEEE. (doi:10.1109/APS.2005.1552172)
61. Graglia RD, Lombardi G. 2008 Singular higher order divergence-conforming bases of additive kind and moments method applications to 3D sharp-wedge structures. *IEEE Trans. Antennas Propag*. **56**, 3768–3788. (doi:10.1109/tap.2008.2007390)
62. Lombardi G, Graglia RD. 2014 Modeling junctions in sharp edge conducting structures with higher order method of moments. *IEEE Trans. Antennas Propag*. **62**, 5723–5731. (doi:10.1109/tap.2014.2355855)
63. Meixner J. 1972 The behavior of electromagnetic fields at edges. *IEEE Trans. Antennas Propag*. **20**, 442–446. (doi:10.1109/tap.1972.1140243)
64. Van Bladel J. 1991 *Singular electromagnetic fields and sources*. Oxford, UK: Clarendon.
65. Chew WC. 1990 *Waves and fields in inhomogeneous media*. Piscataway, NJ, USA: IEEE Press.
66. Harrington RP. 1961 *Time harmonic electromagnetic fields*. New York, NY, USA: McGraw-Hill.
67. Felsen LB, Marcuvitz N. 1973 *Radiation and scattering of waves*. Englewood Cliffs, NJ, USA: Prentice-Hall.
68. Daniele VG, Lombardi G, Zich RS. 2017 Network representations of angular regions for electromagnetic scattering. *PLoS One* **12**, e0182763. (doi:10.1371/journal.pone.0182763)
69. Budaev B. 1995 *Diffraction by wedges*. London, UK: Longman Scient.
70. Lombardi G. 2009 Design of quadrature rules for Müntz and Müntz-logarithmic polynomials using monomial transformation. *Int. J. Numer. Methods Eng*. **80**, 1687–1717. (doi:10.1002/nme.2684)
71. Lombardi G, Papapicco D. 2024 Quadrature of functions with endpoint singular and generalised polynomial behaviour in computational physics. *Comput. Phys. Commun*. **299**, 109124. (doi:10.1016/j.cpc.2024.109124)